POLYMER TUBE EMBEDDED IN-PLANE MICROPUMP: DESIGN, ANALYSIS AND FABRICATION

by

ASHUTOSH SHYAMRAO KOLE

Presented to the Faculty of the Graduate School of

The University of Texas at Arlington in Partial Fulfillment

of the Requirements

for the Degree of

MASTER OF SCIENCE IN MECHANICAL ENGINEERING

THE UNIVERSITY OF TEXAS AT ARLINGTON

AUGUST 2005

ACKNOWLEDGEMENTS

I would like to thank my research advisor Dr. Dereje Agonafer, for his constant guidance, advice and help throughout this project. He helped me develop my thought process and constantly introduced me to the real life problems in the field of MEMS and Microfluidics. I am very much grateful to Dr. Dan Popa for introducing me to this field of research. His constant faith in my abilities was a driving force for my research work. The challenges he put forth for me were helpful to achieve higher goals.

I am thankful to Dr. Raul Fernandez for his faith in me from the beginning of this project. He provided helpful insights through the project.

My special thanks to Dr. Harry Stephanou for introducing me into his team and supporting me constantly.

I am very much grateful to Dr. Jeongsik Sin and Dr. Woo-Ho Lee for the infinite time they spent over me. They are a constant source of inspiration for my work. Their patience and guidance helped me to achieve this goal.

I would also like to thank all my team members for their help. I am grateful to the staff at ARRI and EMNSPC, especially Ms. Kathleen and Ms. Sally.

I want to thank my Parents and sister for their unconditional love and support and the life principles that they installed in me. I would also like to thank all my dear friends for their constant support throughout my life.

July 11, 2005

ABSTRACT

POLYMER TUBE EMBEDDED IN-PLANE MICROPUMP:

DESIGN, ANALYSIS AND

FABRICATION

Publication No. _____

Ashutosh Shyamrao Kole, M.S.

The University of Texas at Arlington, 2005

Supervising Professor: Dr. Dereje Agonafer

This work is aimed at the design, analysis, and fabrication of a novel polymer tube embedded in-plane micropump. A key component of the proposed micropump is a Parylene polymer tube that is embedded into a silicon micromachined structure. The silicon structure composed of active and mechanical components such as an actuator, microchannels, and valves was fabricated using Deep Reactive Ion Etching (DRIE) process with Silicon On Insulator (SOI) wafer. Advantages of embedding a Parylene polymer tube are biocompatibility, thermal and electrical insulation, and leakage free

environments, which are essential requirements for biosensor and drug delivery applications.

The in-plane micropump previously presented faced issues related to the leakage of fluid through the 2 μm gap between the moving diaphragm and the etched out oxide layer at the bottom and the glass cover layer at the top. Inserting a polymer tube can eliminate leakage problems as fluids can only flow the inside of a tube. A biocompatible polymer, Parylene, was used as a tube material because it can be conformably deposited and patterned. The tube itself acts as a diaphragm, which transfers the force and motion of thermal actuators to fluid.

Challenging tasks to realize the proposed micropump are the design and structural and fluidic analysis of a polymer tube coupled with an actuator and the fabrication of a Parylene tub. A multi-physics FEA simulation was performed to guide the design of mechanical structures and thermal actuators of a micropump. The deflection of a polymer tube was used to compute a compression ratio, which determines the flow rate, and back pressure of a micropump. The chemical vapor deposition process was used to conformably deposit 4 μm thick Parylene on the nickel coated DRIE processed silicon wafer, and peeled off and two Parylene layers are bonded together to form a tube. A novel technique of chemical release of the Parylene tube structure from the DRIE mold assisted in the fabrication of tubes with aspect ratio greater that 1:1. Further research is focused on the assembly and packaging of a Parylene microtube to evaluate the performance of the micropump.

TABLE OF CONTENTS

LIST OF ILLUSTRATIONS

Figure Page

LIST OF TABLES

CHAPTER I

INTRODUCTION

1.1 Background

Since the past few decades there has been an enormous growth in research on and development of microfluidics, BioMEMS, Micro Total Analysis Systems (μTAS) and Lab-on-Chip devices. The development of microflow sensors, micropumps and microvalves in the late 1980s dominated the early stage of microfluidics. Life science and chemistry are the main applications of microfluidics [1]. It is research discipline dealing with transport phenomena of fluid based devices at microscopic length scale [1]. With the recent achievement in the Human Genome Project and the huge potential of biotechnology, microfluidic devices promise to be big commercial success. These devices are tools that enable novel applications unrealizable with conventional equipment. With this commercial potential, microfluidics is poised to become the most dynamic segment of the MEMS technology thrust [1]. Microfluidics can now have a revolutionizing impact on chemical analysis and synthesis, similar to the impact of integrated circuits on computer and electronics. Microfluidics will allow the pharmaceutical industry to screen combinatorial libraries with high throughput not previously possible with manual, bench-top experiments. Fast analysis is enabled by the smaller quantities of materials in the assays.

Due to this advances in made in applications, microfluidics devices have improved from its beginnings with the now traditional inkjet print heads and pressure

sensors to a much broader and complex microfluidic handling systems for chemical analyses, consisting of micropumps, valves, flow sensors, separation capillaries, chemical detectors etc, all integrated on a single substrate or as sandwiched modules [3].

All the above-mentioned current and potential application of microfluidics requires handling fluid volumes in order of milliliters and below. These small fluid volumes are often pumped, controlled or otherwise manipulated during operation. Passive mechanisms such as surface tension can sometimes be used for the transport of fluid. For majority of other applications though, microscale pumps, the package size of which is comparable to the volume of fluid to be pumped, is necessary or highly desirable. Thus the micropump is considered the heart of any microfluidic product.

Microscale pumps are usually either mechanical of the membrane type or alternatively the flow is induced by an electric field. New transport effects such as electrokinetic effects, acoustic streaming, the magnetohydrodynamic effect, and the electrochemical effect, which previously were neglected in macroscopic applications, now gain in importance on the microscale [1]. In contrast to other MEMS devices, micropumps are the components with the largest variety of operating principles.

Several review papers present a general overview of micropumps. Gravesen *et. al.* [3] gave a general overview of fluidic problems in the microscale. Many researchers have reported the concept, working, analysis and fabrication of many different kinds of micropumps. Micropumps differ in actuation mechanism, valve mechanism and fabrication process. Pneumatic [5, 9], thermopneumatic [5, 10], piezoelectric [11, 12,

13, 14], electrostatic [9], bimetallic [15], shape memory effect [16] and electrothermal [17] are some of the mechanical actuation techniques presented in past. In the non-mechanical actuation technique electrohydrodynamic [8], electroosmotic [8, 18], ultrasonic [5, 8], magnetohydrodynamic [19] are some of the actuation principles. Passive check valves and dynamic diffuser / nozzle valves form the two major valve principles. The mechanism of transferring the actuation force to the fluid is achieved by ways such as reciprocating motion of the diaphragm or rotary motion of the rotor. Many kinds of materials are being used for fabricating micropumps, silicon being the most common. Brass was used as a material in [25]. Polymers are finding good number of applications as diaphragm materials. Silicone, PDMS and more recently Parylene is used as diaphragms.

1.2 Motivation

Many micropumps designs using silicon are fabricated by microfabrication techniques. They have different parts fabricated on different layers of silicon wafer and then assembled together to form one micropump device. Each layer has a specific function. This type of pumps can handle comparatively large volumes of liquid as the pump chambers and valves are of larger size. Since most of these pumps are made up of silicon and since silicon has a high Elastic modulus, (169 GPa) the pump diaphragm needs to be large for larger deflection and thus the stroke volume and flow rate. Thus the pump chamber is usually large in many traditional micropumps. Fabrication and packaging of these kinds of pump is an issue. Due to large number of layers with different geometric profiles, many complex fabrication steps are involved to fabricate

such pumps. Also the multiple layers require expensive wafer alignment and bonding [17]. This adds to the cost of the device. Even though micropumps are application specific, there are some common parts that are required to make a complete working assemble of the microfluidic system. These parts are the actuator to operate the micropump diaphragm, power circuit to drive the actuator, fluidic reservoir, microchannels for fluidic inlets and outlets and a protective covering to protect form the hazardous environment where it operates under. This leads to large and complex package size and the device becomes bulky and difficult to handle. This makes the microfluidics packaging an expensive process in terms of materials and process. Packaging cost is the major limitation in use of microfluidic and MEMS devices. Moreover, due to the large volumes of fluid handled, there is less control over the flow rate and these pumps are not suitable for very small flow rates.

Many recent applications of microfluidics, particularly in the biomedical area, demand implantable devices, which are biocompatible. Large package size of traditional microfluidic devices makes its implantation into human body difficult if not impossible. Biocompatibility of silicon is also an issue, silicon not being biocompatible.

Piezoelectric actuation method is the actuation technique utilized by many researchers for their micropump devices. Generally piezoelectric actuators require high voltage source, which adds to the cost.

Thus, though the micropumps are widely used recently, its fabrication and packaging cost makes it less viable for general purpose use for a wide variety of applications. The present study makes an attempt to present a design, much simpler and

easy to fabricate and package it for a variety of applications, especially for biotechnology applications where precision control over the flow rate is necessary.

The in-plane micropump design presented in [17] by our group fabricates all the necessary components for a micropump on once single SIO wafer layer. Electrothermal expansion of silicon V beam is the actuation mechanism used in the in-plane micropump design. Lower voltage but high power is used in this actuation technique as compared to the piezoelectric type. The fabrication process is very simple and avoids the use of different and complicated steps. This design allows small diaphragm and pump chamber and therefore precision control of flow rate can be possible.

The present study involves with a modification of the in-plane micropump. The use of a polymer tube as a pump chamber in the present study avoids the contact of fluid and the silicon actuators, thus preventing leakage of fluid. The flexibility of polymer tube can be utilized to for its use a diaphragm material. Critical control over flow rates is possible by changing the geometry of the tube cross-section. The polymer used in this study is Parylene and has many desirable properties such as biocompatibility, conformal deposition and ease of fabrication.

The use of polymer materials in microfluidic devices, in general, ensures precision control over flow rate. Many polymers, including Parylene and PDMS (Polydimethylsiloxane) are being used recently in microfluidic devices, owing to their desirable properties especially for biotechnology area. Processing these materials is also an easy and non-expensive process.

Very few review papers present analysis of Parylene as a structural material. Parylene microchannels were formed and analyzed as a free standing structure and as a wafer bonding material in [32, 39]. Use of Parylene as a diaphragm material is shown in [37, 40]. In the present study, Parylene is used both as a compression chamber and as a diaphragm material. Structural analysis of the Parylene tube is done by applying actuation force over the Parylene tube. Deflections of the tube lead to the pump stroke within the chamber, thus causing pumping of fluid. The fabrication of Parylene microchannels is presented in [32, 39]. Parylene microchannels of aspect ration 1:1 were successfully fabricated in [32, 39], but the process was not suitable to fabricate microchannels with aspect ratio greater that 1:1. A new technique of chemical release of Parylene tube was reported by our group in [8].

Along with the Parylene tube, the electrothermal actuators are also analyzed and optimized for operating temperature to suit the modification in the earlier design. Diffuser / nozzle valve principle is used in the present design. This type of valve eliminates the use of any passive moving valve components. This principle takes advantage of different flow behavior in the diffuser and nozzle direction.

1.3 Approach

Use of Parylene as a structural material is presented the present study. The fabricated actuator deflects the Parylene tube, thus making the tube a combination of compression chamber and diaphragm. Analysis of thin Parylene structure as a diaphragm is presented in this study. Finite Element code ANSYS was used for analysis. Use of symmetry of the tube was made for simplicity of model and accuracy

of calculation, as large number of elements could be used for analysis of a section of the tube. The nodal displacement results were computed from ANSYS, and the stroke volume of the tube was calculated by triple integrating the equation of the deformed surface. This analysis was done to find the compression ratio for various thicknesses.

The modal analysis of the Parylene tube was done to find the natural frequency of the tube, with and without considering fluid in the tube. The purpose of this analysis was to find the type of required analysis i.e. static or dynamic, as the result is used to calculate the flow rate. ANSYS was used to calculate the natural frequency of the tube vibrating in vacuum, and analytical approach was used to find the natural frequency of the tube with fluid on one side. All the above analysis was done for tubes of thickness ranging from 4 μm to 10 μm.

The electrothermal actuators were analyzed to obtain its optimum geometry. The temperature generated in the diaphragm was above the melting temperature of the Parylene tube in the previous design. To decrease the diaphragm temperature, the design of the actuator was modified. This analysis was also done in ANSYS. Coupled elements were used for this purpose to simulate electric, thermal and structural results in one model.

The flow through the diffuser and the nozzle structure and the flow from the pump were determined analytically. A static model was considered for this purpose.

The fabrication process to fabricate the Parylene tube structure is presented in [8] and same method was followed in the present study.

1.4 Contribution

The concept of the in-plane micropump presented in [17] was modified in the present study. The contribution of this thesis includes the proposal of use of a polymer tube as a diaphragm for the in-plane micropump design. A detail structural analysis of the Parylene was done to find the load-deflection relationship. Compression ratio of the pump was calculated from the deformed tube structure. The modal analysis was done to find the natural frequency of the tube for various thicknesses. After the analysis, the dimensions of the Parylene tube was found suitable for application in the in-plane micropump design.

The coupled field analysis of the electrothermal actuator was done in ANSYS to find the optimal working condition. The design was modified to avoid the melting of the Parylene tube upon contact with the actuator. Several final designs, suitable with the Parylene tube design, are suggested in this thesis.

Flow behavior through the diffuser nozzle valves was done using analytical approach. The static assumption was used to calculate the flow rate through the pump.

CHAPTER II

LITERATURE SURVEY

Microfluidic device, Micropump included, is a multidisciplinary research and development field, which covers a broad range of studies including design, modeling, simulation, characterization, fabrication, microflow pattern and phenomenon, etc [1, 2, 3]. Fluid volumes, on the order of a milliliter and below, figure prominently in an increasing number of engineering systems ranging from Biology and Medicine to space exploration and microelectronics cooling [4]. Most initial research in microfluidics resulted in the development of a gas chromatograph at Stanford University, and inkjet printer nozzle at IBM [5]. Since then research in this area has undergone an enormous growth and many different microfluidic devices has been developed, which include valves, pumps, flowsensors, and fluidic mixers as well as chemical and biological sensors [5]. Resent work is mostly focused on integrating several devices on a single substrate, the eventual aim being development of an on-chip chemical analysis system [5, 6].

Microfluidic transportation requirements can sometimes be met by taking advantage of passive mechanisms, most notably surface tension [4]. For other applications, microscale pumps, pressure/vacuum chambers and valves provide adequate microfluidic transport capabilities. Thus micropump research is one of the biggest fields in microfluidics.

2.1 Micropump

As discussed earlier, micropumps play a key role in microfluidic circuits, which are intended to transport very small volumes of fluid for a variety of applications. Dispensing therapeutic agents into the body has long been a goal of micropump designers. Insulin delivery and dispensing engineered micromolecules into tumors or the bloodstream are some of the major research focus for the use of micropumps in the medical field. Precise metering of drug and biocompatibility and not high volumetric flow rate are of great importance here [4]. The pressure generation requirements of the implantable pumps are also significant considering the fact that the backpressure encountered *in vivo* can be as high as 25 kPa. To date, lot of research has been carried out in this area but the number of devices in actual use is not significant. The major hurdles for these systems are reliability, cost, power consumption and biocompatibility [4].

Microelectronic cooling is another major area where micropumps have a great potential of implementation [4, 7]. Micropumps for use in single or two-phase cooling of microelectronic devices are being developed. High flow rate and thus high pressure (100 kPa or greater) is one particular requirement from these micropumps. Cost, power consumption (especially for mobile units) and insensitivity to gas bubbles are some of the critical issues.

Recently much attention is been focused on miniature systems for chemical and biological analysis [4, 5]. These systems have an advantage of reduction in the quantity of sample and reagents required less manual intervention and portability of the system.

In spite of a wide potential for the application of micropumps in these systems, a very limited number of systems are actually there to transport fluids. This limited usage can be due to lack of availability of application specific pumps along with the cost and performance [4].

Space exploration is another exciting area for the use of micropump technology. Miniature roughing pumps are needed for use in mass spectrometer systems to be transported on lightweight spacecrafts. Micropropulsion is another potential application of micropumps in space [4].

The micropumps fall broadly into two categories viz. mechanical pumps with moving parts and non-mechanical pumps [5]. Mechanical micropumps include reciprocating, rotary and peristaltic pumps. Non-mechanical micropumps include electrohydrodynamic, electroosmotic and ultrasonic micropumps [8]. Figure 2.1 shows the classification

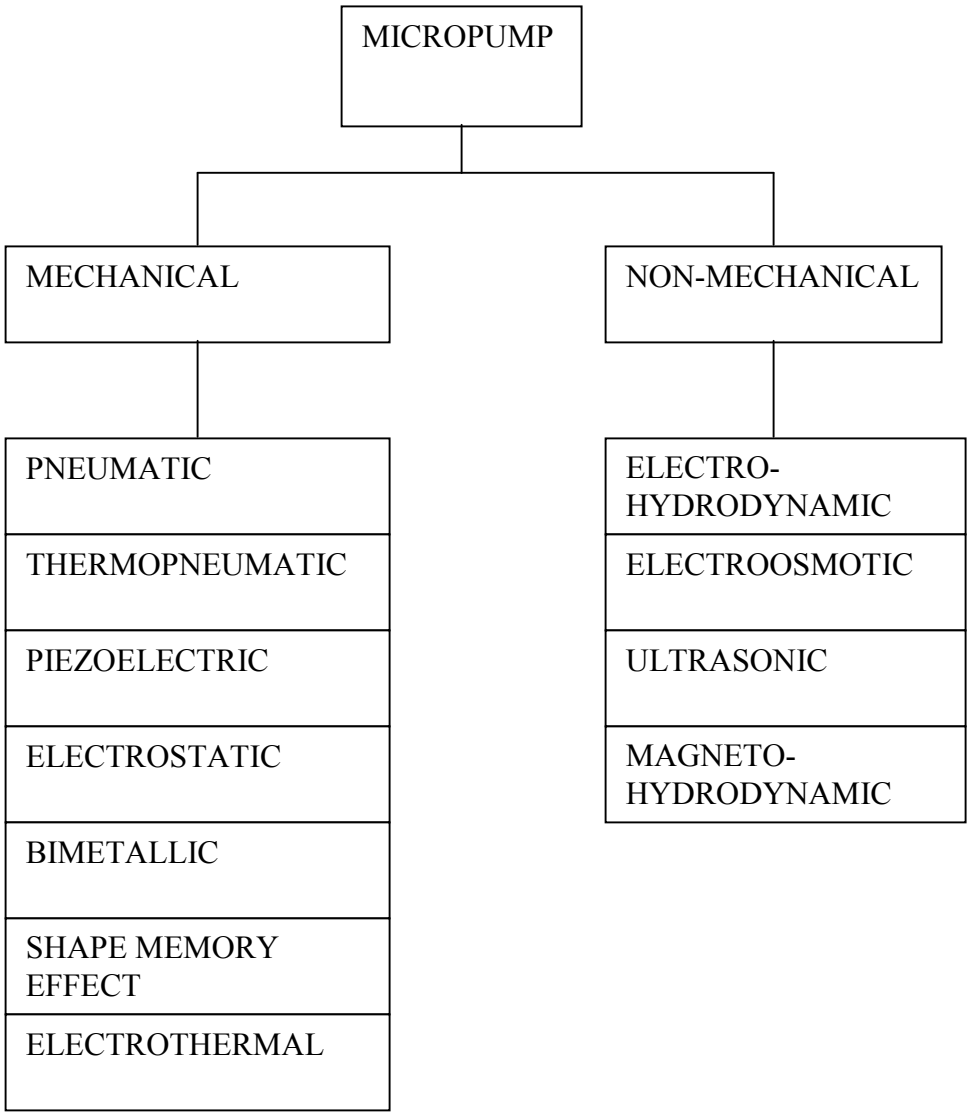

Figure 2.1 Classification of micropumps based on actuation principle.

2.1.1 Mechanical micropump

Mechanical pump or membrane-actuated pump, as it is often known, works of the principle of oscillating membrane creating a varying chamber volume. When the chamber volume increases, the fluid is drawn into the chamber through the inlet valves. When the volume decreases, the fluid is forced out of the pump through the outlet

valve. Here it is essential to have a difference in the flow resistance between the inlet and the outlet for different flow directions [5]. The valves can be cantilever type, membrane type or diffuser / nozzle type. The actuation of the membrane can be carried out in several ways:

In the pneumatic actuation principle the pressure is applied from an external pump on one side of the membrane and thus it deflects the membrane on the other side changing the chamber volume. An external pump source is needed for this type [5, 9].

In the thermopneumatic actuation principle a heated volume deflects the membrane in one direction, whereas cooling releases the membrane tension. Reasonable pump frequency can be achieved if the heated volume is small enough. The heater and the chamber can be fabricated in silicon technology, using bonding of Si-wafer and a heater resistor [5, 10].

Piezoelectric actuation is another very common method of actuation. In this type of actuation a piezoelectric layer is attached to the membrane, such that a change in layer tension leads to the deflection of membrane sandwich [5, 11, 12]. The piezoelectric layer can either surface mounted with conductive epoxy or screen-printed. Sol-gel fabrication [13] in which an organic fluid containing PZT in spun on the wafer and fired at high temperature, and sputter deposition [14] in which a PZT film is created by co-sputtering the correct composition into silicon; are also some means to fabricate the piezoelectric actuator.

In electrostatic actuation technique, an electric field between the membrane and a fixed counter electrode attracts the membrane and thus deflects it. Both the electrodes

can be fabricated using silicon technique and bonding of the two wafers with a predefined space for the two electrodes is possible [5, 9].

In the bimetallic actuation technique, the thermal heat dissipation occurs when a voltage is applied to a poly-Si resistor. Coupled with the aluminum-silicon bimetal effect the heat dissipation in aluminum ring causes a deflection of the whole membrane. This is due to the difference in thermal expansion coefficient between aluminum and silicon [15].

Shape-memory effect is sometimes used as an actuation technique in micropumps. TiNi membrane forms a membrane on two sides of an actuator, deflected in the centre by a spacer. When the top TiNi actuator is heated with resistive heat dissipation, the top diaphragm straightens and deflects the lower diaphragm further. Later, the current is switched off and the bottom diaphragm is heated, so that the opposite movement of the bottom membrane is achieved. When this type of actuator is attached to an inlet and outlet valve system, it can be used for driving fluids [5, 16].

Electrothermal actuation technique uses the principle of electrothermal expansion of silicon V-beam. The silicon beams expand when voltage is applied across it. These beams are attached to the diaphragm through some mechanism and can cause its deflection. This type of actuation provides higher force compared to electrostatic methods but the stroke is not sufficient to achieve desired compression ratio. A lever mechanism is used sometimes to amplify the stroke [17].

2.1.2 Non-mechanical micropump

In this type of micropumps the flow is induced by electric fields. These pumps are quite efficient on micron scale. They often do not have any moving parts, which is an advantage over the mechanical micropumps. Large voltages are however necessary to induce reasonable flow rates. The force produced by an electric field of charged particles causes flow. So if the number of charged particles within the fluid is large, the whole fluid is dragged along due to frictional force. They are again classified according to method of charge generation [5].

The Electrohydrodynamic pumps are based on principle of electric field acting on induced charges in the field that leads to the transduction of electrical to mechanical energy. Thus the fluid properties such as low conductivity and dielectric in nature are significant in EHD pumps [8]. Conventional EHD pumps are based on electric field force and can be classified into injection EHD and induction EHD according to the generation of charges.

In the electroosmotic type the electrokinetic phenomenon of electroosmosis is used for pumping the electrically conductive solutions [5, 8]. If there is double layer of charge between two materials, of which one is a fluid, pumping can be achieved by applying an electric field [5, 18]. The application of electric field leads to a drag in this double layer of ions and causes a bulk motion of the fluid. Switching the voltage without using valves can control the direction of flow. Pumping is in the length of the channel. These pumps sometimes have back flow problems when not pumping due to

absence of valves to check it. Also large amount of electrical input is needed to generate the necessary field strength [8].

The ultrasonic types of micropumps work on the principle of acoustic streaming, which is the motion of fluid upon the application of finite amplitude acoustic field [8]. These micropumps are mainly intended for moving fluids along a surface and not through pipes and whole system of channels and microfluidic devices [5]. The acoustic wave is set up by using Flexural Plate Wave (FPW), which in turn is generated by piezoelectric actuators. These pumps have an advantage of low operating voltages and no need of valves. Also there is no dead volume associated with the pump, as the channel itself is the pump. However there are back flow problems once the pumping action is stopped.

Magnetohydrodynamic type of non-mechanical actuation technique is sometimes used in microfluidics. The working principle of MHD pumps is the pumping force is exerted ion the electrically conductive fluid flowing through magnetic and electric fields [19]. The structure is simple which is made up of microchannels with two electrodes at the ends to apply electric fields and two walls of the microchannels are bounded by two permanent magnets of opposite polarity that exerts a magnetic force [8]. The liquid in the channels moves due to Lorentz force that is applied to the fluid in the direction perpendicular to both the electric field and magnetic fields. These types of pumps allow fluids with greater conductivity to be pumped and thus allow for it to be used for medical and biological applications. These are also simple to fabricate and have bi-directional pumping capability.

2.2 Diffuser / Nozzle Micropump

Diffuser / nozzle type of micropumps are often called valve-less micropumps. This type of micropumps does not incorporate any kind of passive valve mechanism to direct the flow. Instead, the property of differential flow through the diffuser and the nozzle is used to create a unidirectional flow. Actually there will be flow through both inlet and outlet valves during pump operation but there will be a preferential flow in either diffuser or the nozzle direction depending on the taper angle. For smaller taper angles, the diffuser direction is the preferred direction of flow while for larger taper angles, the nozzle direction is the preferred direction of flow [5]. The advantage of using this kind of valve principle is that there are no moving parts involved. This will eliminate the wear and fatigue of the components. The device will be reliable and will have a longer life. This is of particular importance for biomedical applications. There will be no clogging of pump due to particle leaden fluids. Moreover these pumps are easy to manufacture.

Stemme [25] has presented the first prototype of such a pump. This design was machined in brass and was rather large for MEMS applications [5]. This pump allowed both water and air to be pumped at reasonable flow rates and backpressures. Later Olsson *et. al.* [11] from the same group presented a piezoelectrically actuated pump based on microfabrication techniques. Recently, the same group has presented a dual chamber diffuser / nozzle micropump based on microfabrication techniques [42]. The use of dual chamber reduced the effect of ripples during the pump strokes. The common characteristics of the above mentioned pumps was that in all the pumps, the taper angle

of the diffuser / nozzle structure was rather small, making the diffuser as the preferred direction of flow as compared to the nozzle direction.

Gerlach [26, 46] presented a piezoelectric actuated membrane pump with KOH etched diffuser / nozzle valves. The angle of taper for the diffuser / nozzle was around 35.4°, which made the nozzle direction as the positive direction of flow. This pump was also based on microfabrication techniques.

2.3 Analytical work

Most of the published work on microfluidic components includes fluid mechanic modeling as a design tool, or as a way to correlate and explain experimental results. In many cases, the flow-pressure characteristics of a device are dominated by one single restriction, and it is sufficient to use a simple analytical model well known from macroscopic fluid mechanics [3].

Numerical simulations are used in the case of more complex structures or systems [20]. The most common method of numerical simulation is based on a subdivision of the complete structure into lumped elements, which can be described individually by simple analytical models, and for which simple relations between individually lumped elements can be formulated. These models and relations of interaction can then be fed into a dedicated or generally available computer program. In this way, micropumps have been simulated using a so-called Bond graph simulation tool [3].

The precondition for successful fluid mechanic modeling using direct analytical models or lumped elements models relies on correct assumptions as to type of flow [3].

In order to determine whether a given flow pattern is laminar or tubular, it is common practice to evaluate the Reynolds number and compare it to the transitional number 2000 or 2300.

The most accurate method of modeling is probably to use the concept of continuum theory, which couples the relevant mechanical, electrodynamic, and thermal field quantities in terms of a system of partial differential equations [20]. This approach can be implemented using finite element programs. The problem is that for a realistic system the model is very large and hardly possible to solve due to the required computer power [21]. The usual approach is instead to use a lumped-mass model to describe a system, e.g., a micropump. This is based on subdivision of the complete structure into lumped mass elements which can be described individually by simple analytic models and for which simple relations between the individually lumped elements can be formulated [3]. This approach has been used in several works [21].

The operation of reciprocating displacement micropumps often involves the interaction of several types of mechanics including electromechanical forces, solid mechanics and fluid mechanics. Because of this complexity, accurate, tractable, broadly applicable analytical models of reciprocating displacement micropump operation are not readily available. Low-order lumped-parameter models provide significant insight on key aspects of micropump operation [4, 20]. Finite element analysis is also a useful tool in studying reciprocating displacement micropumps. Commercial packages such as ANSYS and ALGOR have been used to analyze the response of micropump diaphragms subjected actuator forces [4, 20]. A variety of numerical and semianalytical

approaches have been taken in the study of fluid flows in reciprocating displacement micropumps [4, 22, 23]; commercial packages suitable for such analysis include CFDRC, Coventor, FEMLAB and ANSYS FLOTRAN [4, 5, 24].

2.3.1 Analysis of Diffuser / nozzle micropump

A mathematical model that can simulate the pump performance under given geometrical and operational conditions is essential for the optimal design of diffuser / nozzle pumps. Most of the previous models were based primarily on kinematical considerations. That is, the flow rate was calculated based on a known volume displacement caused by the movement of the piezoelectric membrane (Stemme and Stemme [25] Gerlach *et al.* [26] Olsson *et al.* [11] Heschell *et al.* [27] Olsson *et al.* [28] and Ullmann [29]). These models are quite useful; nevertheless they are incapable of predicting the dynamic behavior of the pump. Recently Olsson *et al.* [20] and Ullmann *et al.* [30] modified the kinematic model by taking into consideration the acceleration of the fluid in the nozzles. An improved dynamic model for determining the dynamic behavior of the piezoelectric pump is presented in [31]. It takes into account more accurately the effect of the inlet and outlet lines. Namely, no approximation is made concerning the frictional and accelerational pressure drop in the leading pipes both for the calculation of the natural frequency and the calculation of the pump performance. There are several advantages to this model. It is based on straightforward momentum equations. It is able to simulate the complete behavior of the piezoelectric pump. It can be used to calculate the pump efficiency as well as the effect of the driving frequency and the inlet/outlet lines on the pump performance.

2.4 Parylene properties and use

Parylene is a highly crystalline, straight chain polymer. Unlike other polymeric materials, it is not manufactured or sold as a polymer, but rather is produced by vapour-phase deposition and polymerization of para-xylylene. The method of Parylene deposition is called condensation coating. The Parylene get conformally coated over all areas, edges, points and internal areas. With Parylene the object to be coated remains at or near room temperature eliminating all risk of thermal damage.

Parylene is extremely resistant to chemical attack, exceptionally low in trace metal contamination, high dielectric strength, high mechanical strength, very high surface and volume resistivities, and other superior electrical properties that remain virtually constant with change in temperature. Its high reliability makes it suitable for military and commercial applications. Parylene is insoluble in common solvents and is acid and base resistant. It is also fungus and bacteria resistant. Perhaps the most important property of Parylene is its biocompatibility, making it suitable for medical and biological applications.

In current commercial applications, Parylene is deposited in thickness ranging from a thousand angstroms to about 75 microns depending on the function that Parylene film has to perform. The thickness can be controlled generally to plus or minus 10%. Also Parylene requires no catalysts or solvents thus eliminating environmental concerns. Parylene has a glass transition temperature of 90°C and a melting temperature of 290°C [32]. Parylene can work in a wide range of temperature ranging from - 200°C to + 200°C.

The coefficients of static and dynamic frictions for Parylene are virtually the same and are very low. Thus Parylene can serve as a "dry film" lubricant, which aids greatly are devices such as miniature servomotors. The Parylene coating is light eight as compared to other coatings and is transparent, making the thin films of optical quality.

Parylene C is poly-monochloro-para-xylylene, and is most widely used type of Parylene. It has excellent barrier properties, low permeability to moisture and gases, such as nitrogen, oxygen, carbon dioxide, hydrogen sulphide, sulphur dioxide and chlorine while retaining excellent electrical properties.

2.4.1 Parylene applications

Biocompatibility along with the fact that Parylene can be patterned by using oxygen plasma makes it extremely suitable for MEMS applications [33]. High mechanical strength and chemical and solvent resistance are also favorable properties of Parylene. Some of the applications of Parylene are discussed below.

2.4.1.1 Flow sensor

The application of Parylene as a flow sensor is described in [34]. Here the Parylene MEMS thermal sensor array is capable of detecting small flows down to 0.5 µl/min. An array of metallic sensing elements made of platinum is sandwiched in Parylene membrane. The device is fabricated using low-temperature Parylene/platinum technology and consists of metallic sensors suspended on a membrane over a bulk micromachined silicon channel [8, 34]. An array layout is utilized to determine the flow direction as well as the thermal profile in the fluid. Parylene is chosen here as the membrane material as it is transparent and biocompatible.

2.4.1.2 Flow control actuator

Flexible Parylene membrane was used as an electrostatic actuator for flow control [33]. The membrane was electrostatically actuated to act as valves and achieve flow control by patterning the Parylene membrane and deposition of metal electrodes.

2.4.1.3 Micro check valve

A micro check valve design was made using Parylene. It features a bulk-micromachined valve seat (with an orifice) and a new twist-up tethered Parylene-membrane [35]. The twist-up tethers allow large membrane displacement, and thereby reduce membrane-induced flow resistance to a negligible level.

2.4.1.4 Gas chromatography

Parylene microchannels have been fabricated for gas chromatography applications. An embedded heating element is fabricated to heat the gas flowing through the parylene microchannels [36].

2.4.1.5 Parylene as a wafer bonding material

Parylene-Parylene bonding can take place at temperatures close to the melting temperature i.e. 290°C. The bonding takes place by chain inter-diffusion between Parylene layers. This phenomenon was reported in [32, 39]. The bonding was tested for shear and leakage and was found that it survived the tests. It was reported that temperature is a dominant factor than pressure and time. Good bonding results were obtained at temperature above 190°C with pressure of 24 MPa. This temperature is between the glass transition temperature and melting temperature of Parylene. Since the bonding temperature is lower that the melting point and since Parylene is a crystalline

polymer, only a small amount of short amorphous chains can be mobilized and contribute to the bonding via inter-diffusion at the Parylene-Parylene interface [32, 39]. The heating is usually done by variable frequency microwave energy. The advantage of this bonding technique is short bonding time, low bonding temperature, relatively high bonding strength, less void generation and low thermal stress [39].

2.4.2 Parylene analysis

Traditionally Parylene has been used to form an insulating thermoplastic coating on electronic devices. However, recently Parylene has drawn considerable attention as a structural material for microfluidic devices because of its excellent mechanical properties, chemical inertness, biocompatibility and stress free conformal deposition. Many recent applications have been reported including plane and corrugated diaphragms [37] and Parylene microchannels [32]. These are thin film structures which are either fixed to the substrate or free-standing. Structural analysis followed by experimental verification was done to test the use of Parylene as a structural material.

Finite element method was employed to analyze mechanical behavior of Parylene diaphragm in [37]. Thermal and load-deflection finite element analysis of flat and corrugated Parylene diaphragm was performed to find an effect of the residual stress on the stiffness of the diaphragms. The simulation showed that the mechanical sensitivity of the diaphragm is greatly influenced by residual stress caused by the thermal process (silicon wet etching). The finite element analysis results that took residual stress into account matched with the experimental results.

A new fabrication technique of enclosed Parylene microchannel was presented in [32]. Parylene microchannels of different cross sections were molded and formed by depositing Parylene into silicon mold and then covering it with another layer of Parylene, followed by bonding to two Parylene layers. In this way Parylene tubes of aspect ratios of 1:1 were successfully formed. ANSYS 2D modeling was used to analyze these tubes for internal pressure – deflection relationship. The pressure represents the pressure generated by flow. It was observed that no significant deflection occurred for Parylene thickness of 10 μm and applied internal pressure of 10 psi [32].

CHAPTER III

IN-PLANE MICROPUMP DESIGN

This study is based on the previous pump design called In-plane Micropump [17]. This design had all the necessary components such as diaphragm, valve, actuator etc. fabricated on a single silicon layer, using Deep Reactive Ion Etching (DRIE) process.

3.1 Initial design, fabrication and analysis of In-plane micropump

Most of the micropumps existing today are made up of multiple stacked layers and each layer has a single function such as a diaphragm, a valve or an actuator. This kind of design requires wafer bonding with precise alignment and an external actuator will also be needed to operate this pump. Therefore the fabrication of such pumps can usually require multiple steps and can be complex and thus the fabrication cost increases.

3.1.1 In-plane micropump

The in-plane micropump design has all its key parts i.e. the actuator; pump diaphragm and the valves fabricated in a single silicon substrate. This design makes fabrication of the pump much simpler and thus reduces the cost. Due to the compact size and small diaphragm, precision flow rate can be achieved. This pump is based on the actuating principle of electrothermal expansion of silicon thin ribs, also called V-beam. The actuators are embedded into the pump. When the electrical voltage is

applied to the actuator, the V-beams expand by means of Joule electrical resistance heating. The force generated caused by the rib's expansion pulls or pushes the rigid bar that is pivoted by a thin flexible bar. The flexible pumping plate is attached to the silicon V-beam and move linearly along the surface of the wafer. Two such actuators are placed facing each other. A stroke amplification mechanism is adopted to minimize the driving power and improve the compression ratio of the pump. A lever structure is used for this purpose. This is an advantage over other out of plane micropumps where the actuators are generally external to the pump structure.

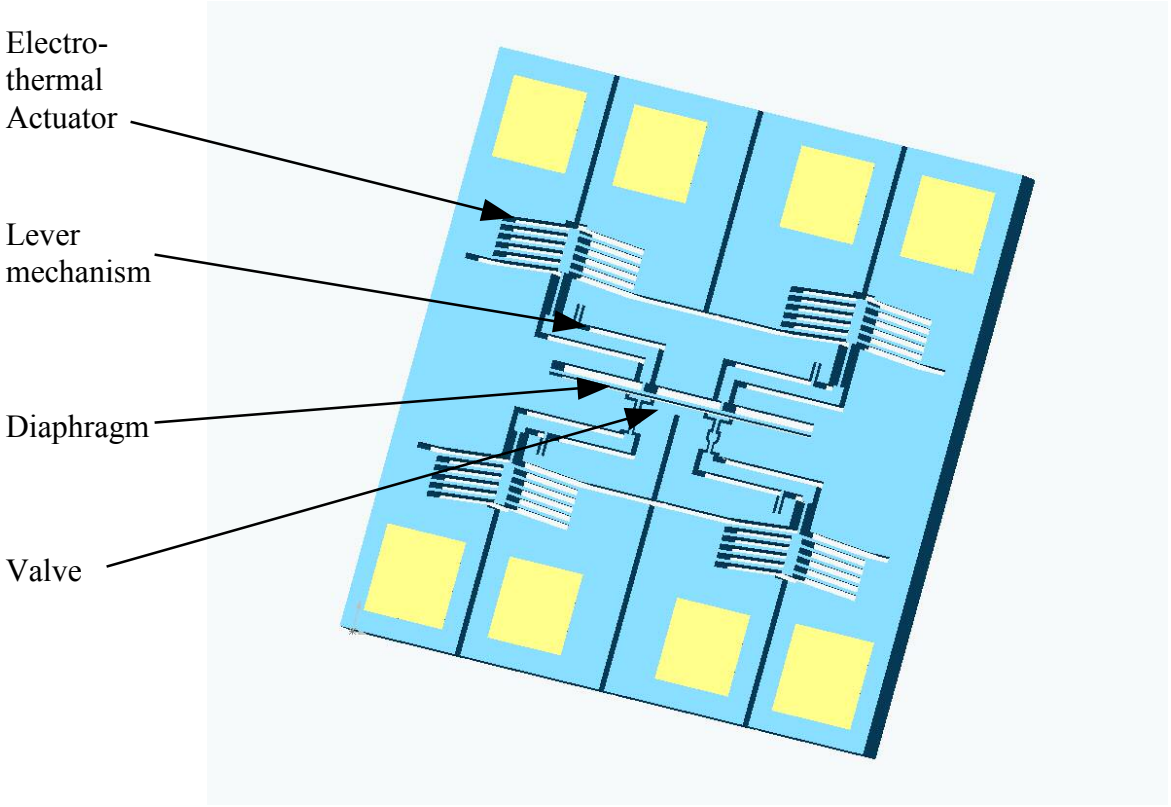

Figure 3.1 In-Plane micropump.

Either check valves or diffuser / nozzle valves are used with the diaphragm to direct the flow. In the diffuser / nozzle case, the flow path gradually increases at the inlet port and gradually decreases at the outlet port. The flow resistance is low in the diffuser direction than in the nozzle direction incase the taper angle is small (< 10°). During the suction stroke, the inlet is the diffuser direction and the outlet is the nozzle direction, and during the compression stroke, the inlet is the nozzle direction and the outlet is the diffuser direction. Thus there is a resultant fluid flow in the outlet direction with repeated diaphragm motions. Cantilever check valves are passively operated by pressure difference between chamber and the ports. At the suction stroke the inlet check valve will open while the outlet check valve will close and the opposite takes place at the compression stroke.

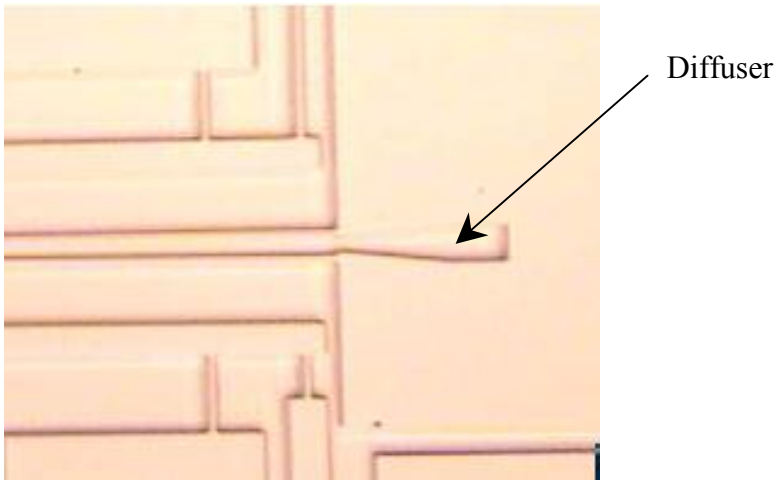

Figure 3.2 Diffuser / Nozzle valve in the In-plane micropump.

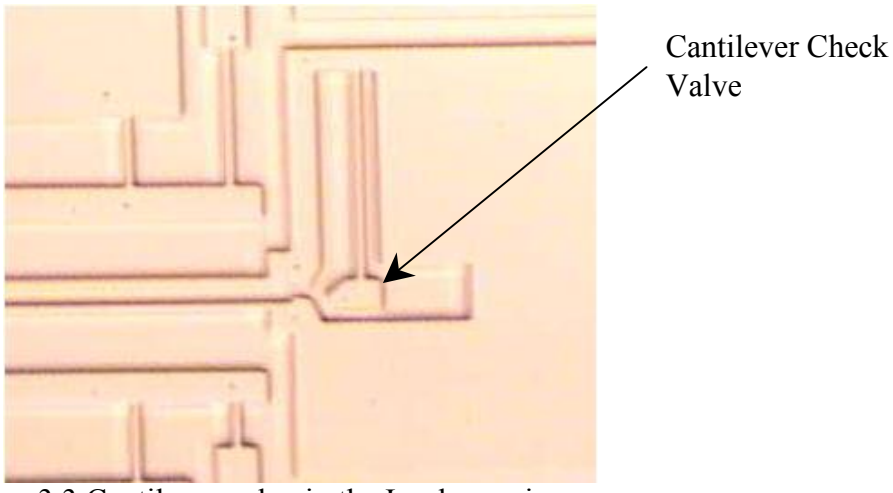

Figure 3.3 Cantilever valve in the In-plane micropump.

Deep Reactive Ion Etching (DRIE) is used to fabricate the pump structure on Silicon On Insulator (SOI) wafer. The pump performance is estimated by the characterizing the electromechanical properties and is documented in [17]. The pump die was anodically bonded with the glass plate to enclose the fluidic flow passages. To accommodate for the moving parts in the pump layer, a few micron gap was provided between the pump and the glass plate. The glass plate had through hole for electrical interconnections of the pump.

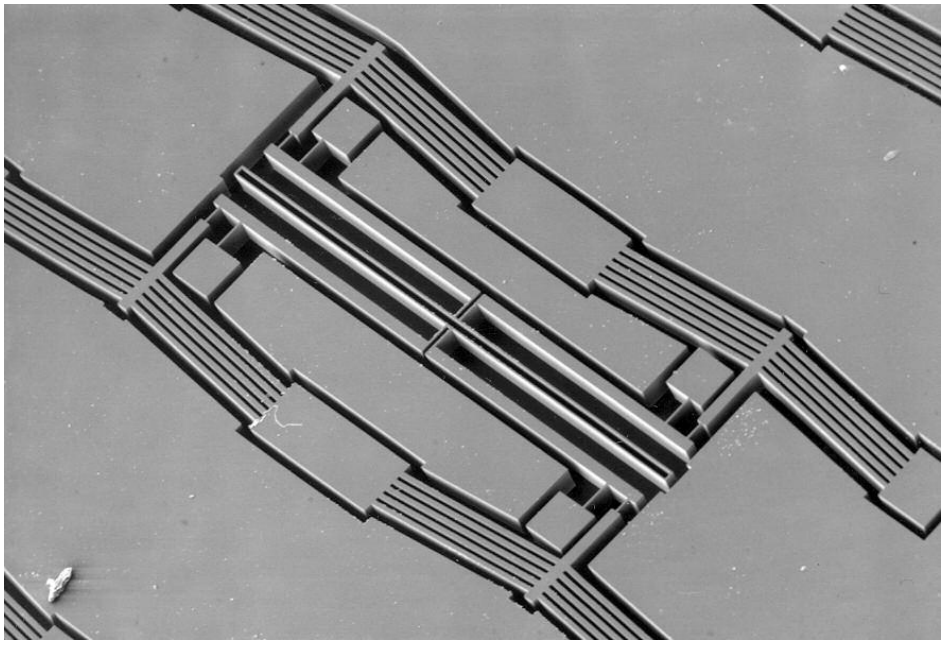

Figure 3.4 Deep Reactive Ion Etched micropump structure on SOI Wafer.

3.2 Improvements in the initial design

The in-plane micropump design had some design issues related to leakage of fluid. The top glass plate formed a cover over the pump die. There was a small gap of approximately 2 μm provided between the top cover and the pump die. This was done to accommodate the motion of the moving parts i.e. actuator, diaphragm, and check valves. The flow passage of the fluid was from the inlet valve through the pump chamber and towards the outlet through the outlet valve. The fluid was pressurized in the pump chamber by the in-plane motion of the diaphragm.

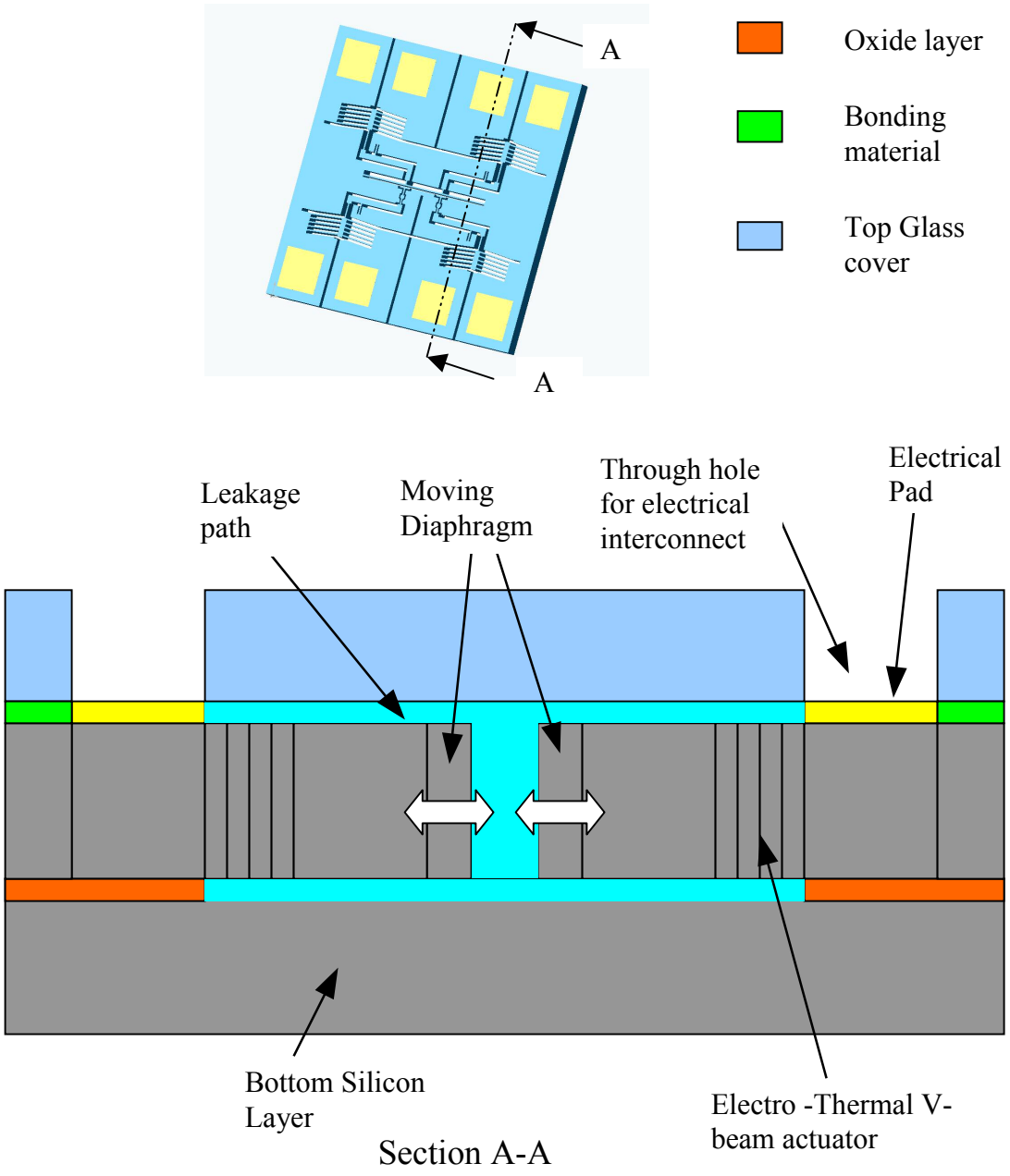

Figure 3.5 Schematic of cross section of the micropump showing the leakage pattern.

Thus majority of the fluid would move towards the outlet valve, but due to the gap provided between the pump die and the top cover plate, some fluid would also leak

through this gap. After leaking, the fluid would ultimately reach the electrothermal V-beam actuator and other electrical connections. This would stop the functioning of the pump. Figure 3.5 shows the cross section view of the flow through the diaphragm and the leakage pattern.

3.3 Use of a Polymer Tube

There is a need to avoid the water from getting to the electrothermal actuator and the electrical connections so as to operate the pump. A new concept is to physically separate the fluidic circuit from the rest of the pump silicon structure. For this the fluid needs to be enclosed in some kind of a flexible tube running between the vibrating actuators. The tube needs to be flexible so as to bend upon the contact with the actuator and transmit the force to the fluid enclosed within. At the same time the tube needs to have enough strength so as to sustain the deflections caused by the moving actuators and the inner fluid pressure. Also the tube needs to be of an insulating material so as not to transmit the heat from the thermal actuators to the fluid enclosed. The tube structure needed to fit in a narrow trench like structure in between the silicon v-beam actuators. The length is large as compared to width and height. For this purpose, the tube should be a thin-film structure instead of bulk structure. At the same time it should be manufacturable. This is particularly a challenge because of the small size of the tube and that the current tube manufacturing process would not support manufacturing of such small tubes. Altogether, the selection of the tube material and then the manufacturing process is a challenge.

Upon extensive literature search it was found out that a polymer Parylene can be a suitable material for this kind of a tube structure due to its physical properties and the fact that it's a thin-film structure. Polymeric materials are more flexible and ductile than silicon or dielectric materials [38]. The properties and applications of Parylene are discussed in Chapter II. Parylene has excellent mechanical properties i.e. high tensile and yield strength compared to other polymers. But at the same time it is flexible enough to deform under application of comparatively small loads. The Young's modulus of Parylene is around 3 GPa, which is 70 times less than Silicon. Parylene tube is also biocompatible. This is of particular importance, as the micropump can be used in applications as either a biosensor or as an implantable drug delivery system. Chemical inertness is also another useful property. Polyimide and PDMS have a high permeability to liquids and gases as compared to Parylene [38]. The main advantage as far as manufacturing of such a tube is concerned is that Parylene can form stress free conformal coating of uniform thickness. The coating method is such that the there is no intermediate liquid stage in coating and it takes place from a gaseous monomer. As a result the component configurations with sharp edges, points, flat surfaces, crevices or exposed internal surfaces are coated without voids. The process is also cost effective.

The process employed to develop this kind of a tube is called 'Parylene micromolding'. In order to fabricate a tube the coating of Parylene is done in two steps and the two layers thus formed is joined together by thermal bonding process. The bonding takes place at some temperature below the melting temperature of Parylene, which is 290°C. This process is reported in [32]. Parylene is deposited on a mold and a

flat surface, and then the molded Parylene is released from the mold and bonded to the flat Parylene layer, forming a free standing tube like structure.

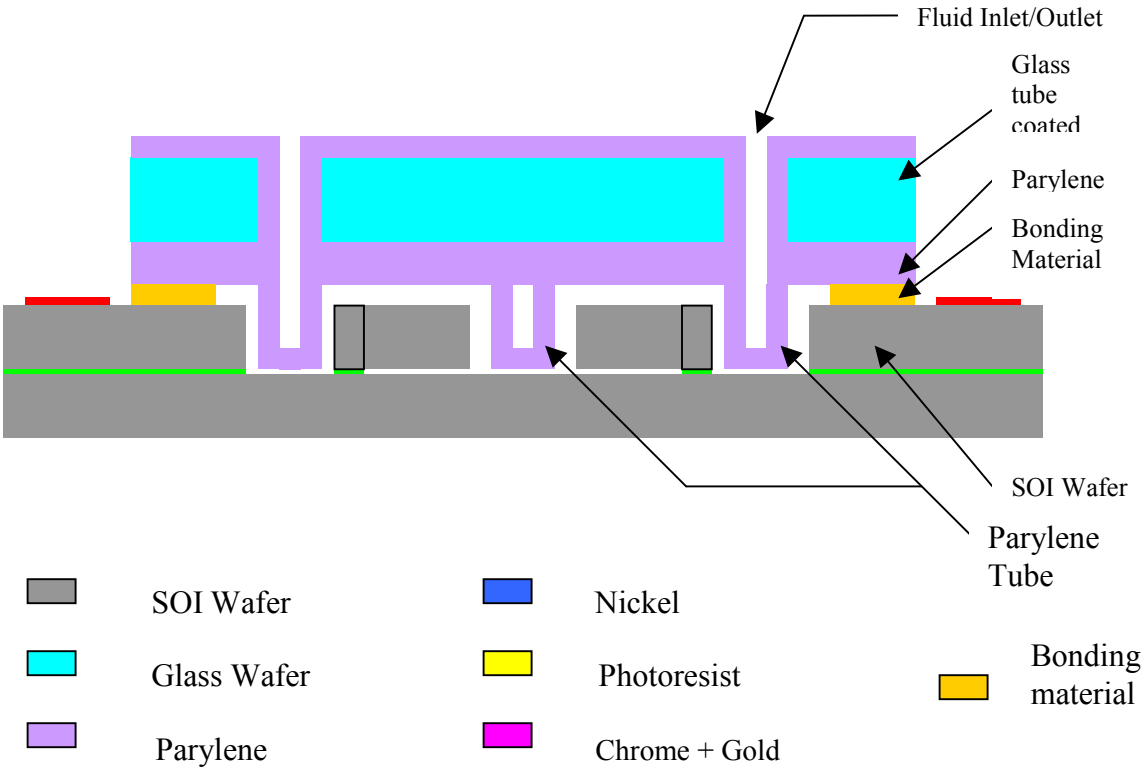

Figure 3.6 Schematic of cross section of the pump showing the design modification including the Parylene tube structure.

The final structure thus formed is a fully enclosed channel structure in Parylene, and a part of which acts as a diaphragm while being actuated by the electrothermal v-beam actuators. Figure 3.6 shows the cross section of the modified design of the in-plane Micropump including the Parylene structure.

The fluidic inlets and outlets are formed by etching the top glass cover followed by depositing Parylene over it. This Parylene coated glass top plate is then aligned and bonded with the molded and released Parylene structure, which is formed in a silicon

mold. This Parylene-Parylene bonding takes place at a temperature just below its melting point. The process is explained in Figure 3.7 and the whole technique will be discussed in Chapter V.

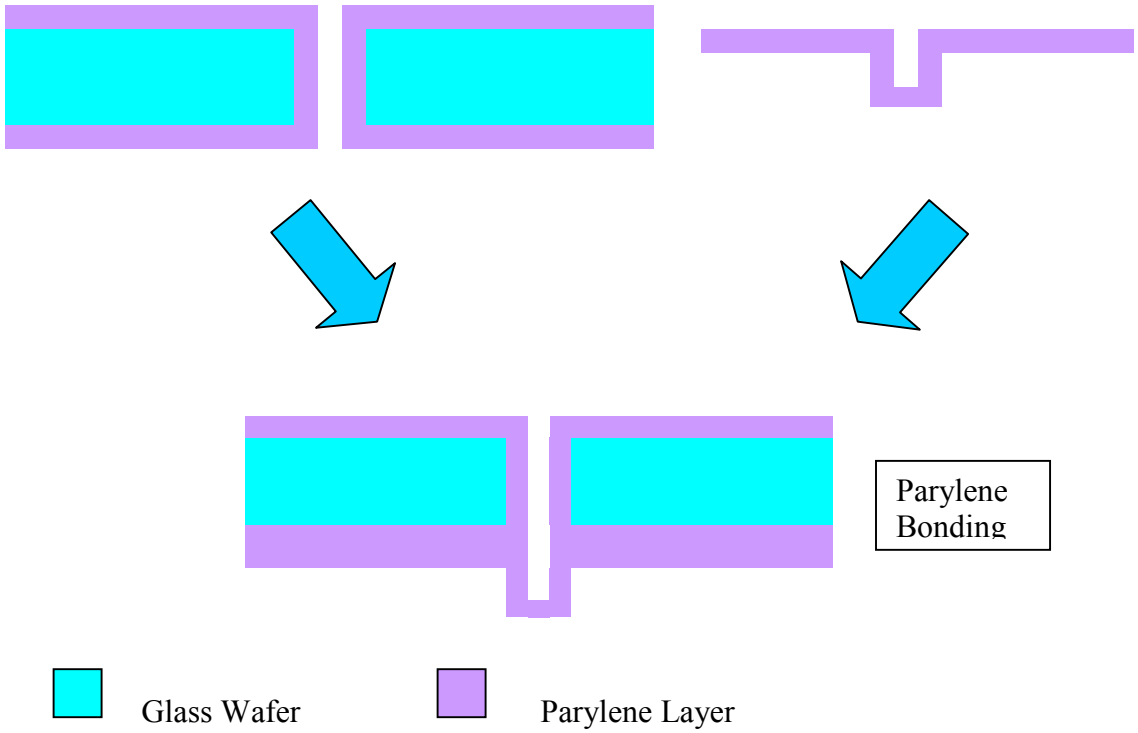

Figure 3.7 Schematic of cross section of the top glass cover plate being bonded with free standing Parylene structure.

CHAPTER IV

ANALYSIS OF POLYMER TUBE MICROPUMP

Parylene is traditionally being used as an insulating material as thermoplastic coatings on electronic devices. However, recently it has drawn considerable attention as a structural material in MEMS and microfluidic devices. This is owing to its good mechanical properties, chemical inertness, optical transparency and low permeability to moisture and gases. But the two most outstanding properties of Parylene, which make it stand out from other polymers, are its biocompatibility and conformal stress-free deposition. Some other properties are high reliability, wide temperature range – ranging from - 200°C to + 200°C, solvent resistant, high dielectric strength, low coefficient of friction, light weight, fungus and bacteria resistant, radiation resistance and high surface and volume resistivities. Most of the properties of Parylene remain constant with changes in temperature.

Due to these outstanding properties, considerable numbers of MEMS and microfluidic devices have been developed with Parylene utilized in it for some particular function. Flow sensor [34], flow control actuators [33] and micro check valves [35] make use of Parylene as a structural material. Parylene was also used in gas chromatography [36] where Parylene microchannels were formed as a freestanding structure and as a wafer bonding material [32, 39] where its bonding strength was tested and found to be good. Use of Parylene as a diaphragm material is shown in [37, 40],

where; mechanical behavior of flat and corrugated diaphragms was analyzed using finite-element method. Parylene was successfully used as a diaphragm material and the load-deflection relationship was studied for both flat and corrugated diaphragms. The focus of study was to determine the effect of thermal residual stresses in the diaphragms, which were caused by the thermal process of silicon wet etching. In their process, first the silicon wafer was oxidized followed by corrugation generation on the wafer. Then Parylene was deposited and then the wafer was backside etched using ethylene diamine pyrocatechol (EDP). This process took place at around 70°C. Due to the difference in thermal expansion coefficients of Parylene and silicon, thermal residual stresses were developed in Parylene which made the diaphragm difficult to deflect.

The Parylene deposition process employed in this thesis is free of any thermal residual stresses. Parylene is deposited over DRIE silicon molds, which are already deposited with Nickel or are oxidized. This process takes place at room temperature. The Parylene layer is then chemically released by etching away the Nickel or oxide layer with respective enchants. Both these etching processes take place at around room temperature, and the Parylene is not exposed to high temperatures.

A method of enclosed Parylene microchannel fabrication was proposed in [32]. Here, free standing Parylene microchannels were fabricated by depositing Parylene over DRIE silicon molds. This Parylene structure was then released by using releasing agents such as Micro-90 (Specialty Coating Systems) and Camie 1080 (Camie-Campbell Inc., St. Louis, MO). With this technique, Parylene microtubes of various cross-section

geometries were formed. There was a limitation on the height of microchannels fabricated. It was inferred that with the present releasing technique, a tube of aspect ratio (width:depth) 1:1 was easy to release. This method of releasing was not suitable for aspect ratios higher than 1:1. [32]. ANSYS 2D was used to analyze these microchannels for pressure-deformation relationship. Bonding method developed in this report confirmed a leak free path.

The fabrication process applied in this thesis can manufacture microtubes with aspect ratio greater that 1:1. The high aspect ratio of the microtube is achieved by using chemical removal of the sacrificial metal layer between the mold and Parylene tube. Tubes with aspect ratio of about 1:3 have been fabricated and reported in [8].

4.1 Parylene tube analysis

The flexibility of the tube material, Parylene, makes it suitable to deflect upon contact with the electrothermal V beam actuator. Two electrothermal actuators are placed facing each other and the Parylene tube is placed in between them. The two actuators push the tube simultaneously upon application of voltage across its pads. The tube deforms transferring the pressure from the actuator to the fluid it encloses. The diffuser / nozzle valves cause a resultant flow in one direction. There are three types of Parylene generally used. Those are Parylene N, Parylene C and Parylene D. The type of Parylene used in this study is Parylene C. Parylene C has a useful combination of electrical and physical properties plus a very low permeability to moisture and other corrosive gases. Along with its ability to provide a true pinhole free conformal

insulation, Parylene C is the material of choice for coating critical electronic assemblies. The mechanical properties of Parylene C are given in the following table.

Table 4.1 Physical and Mechanical properties of Parylene C.

Properties		**Parylene C**
Young's Modulus (Pa)		2.75×10^9
Tensile Strength (Pa)		6.89×10^7
Yield Strength (Pa)		5.51×10^7
Elongation to Break (%)		200
Yield Elongation (%)		2.9
Density (kg/m^3)		1289
Index of refraction (n_o^{23})		1.639
Water Absorption (% after 24 hours)		< 0.1
Rockwell Hardness		R80
Poisson's Ratio		0.4
Coefficient of Friction	Static	0.29
	Dynamic	0.29

As stated earlier, Parylene is a thin film material. It can be conformally deposited over a substrate to acquire its shape. After chemical release of this Parylene layer, a freestanding structure of Parylene is obtained. A similar process is applied in the present study to form freestanding Parylene microtube. The Young's modulus of Parylene is 2.75 GPa, which is 70 times less than that of Silicon (190 GPa). This makes

the tube flexible and yet with enough strength to be used as a structural material. Thus the tube can easily deflect upon application of pressure. The cross-section of the tube is represented in Figure 4.1.

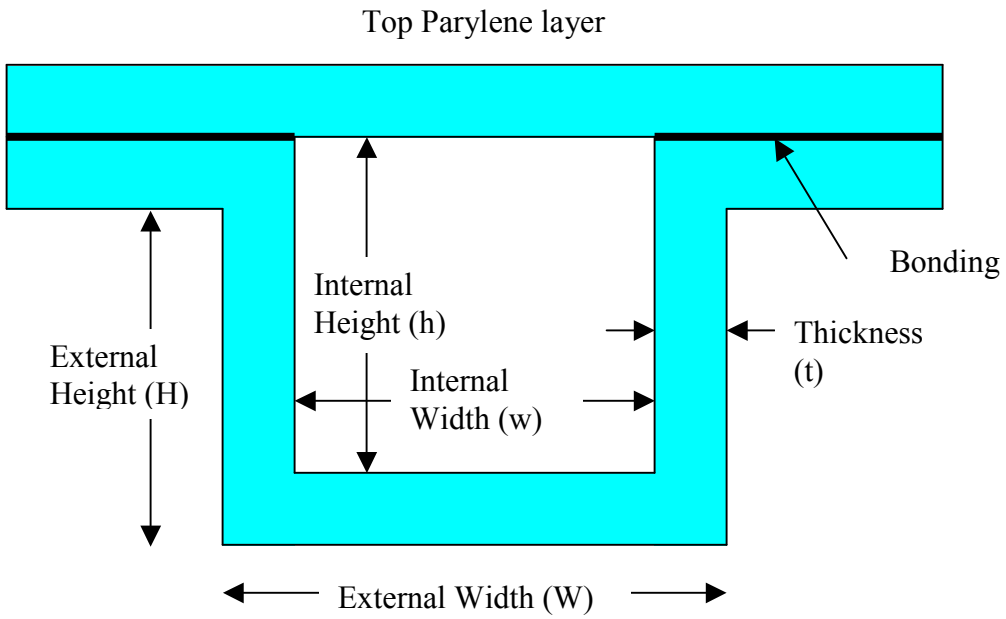

Figure 4.1 Schematic cross-section pf the Parylene tube structure showing the top and the bottom parts bonded together.

As the cross-section geometry i.e. width and depth, of the DRIE structure for the tube section remains the same, the External Height (H) and the External Width (W) will remain constant irrespective of the Thickness (T) of the tube. This is because the Parylene gets conformally deposited over the DRIE structure. The thickness of the tube will vary upon the deposition time and rate of Parylene during the deposition process. The thickness will therefore control the internal volume of the tube if the length of the tube remains constant. The present cross-section of the tube is square shape. This shape remains the same irrespective of the thickness (t) of the tube. Only the cross-section

area changes along with the thickness (T) for a given DRIE mold. In the present study both the external height (H) and the external width (W) of the structure are taken as 100 μm.

The whole internal volume of the tube acts as the pumping chamber with the walls acting as the diaphragms. The electrothermal V-beam actuator actuates the sidewalls of the tube as shown in Figure 4.2. The detailed assembly is shown in Figure 3.3.

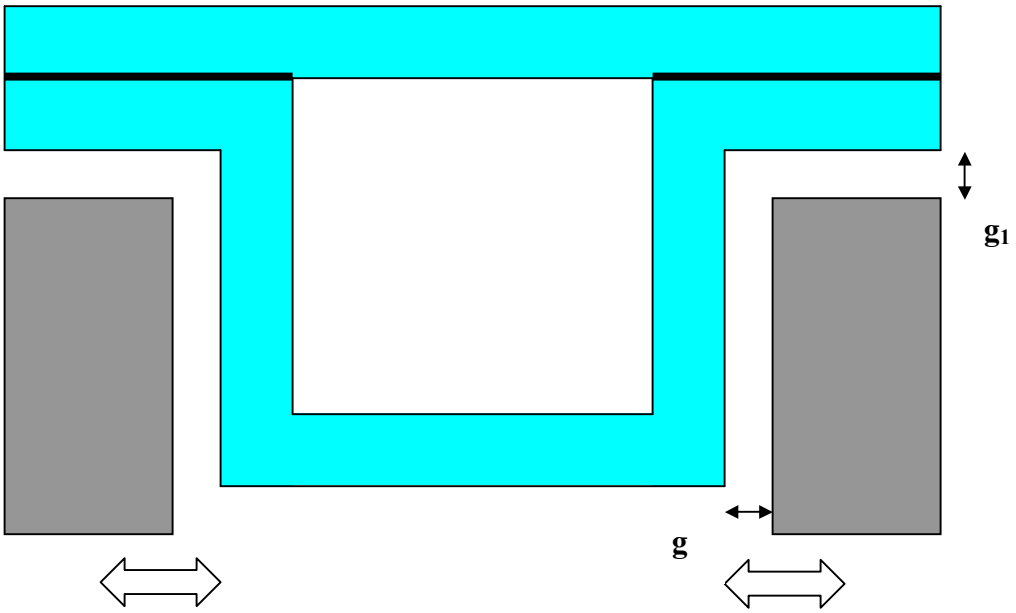

Figure 4.2 Schematic cross-section of the Parylene tube showing the position of the electrothermal actuators.

The Figure 4.2 shows the position of the actuators with respect to the Parylene tube when the actuator is not operating. At this state of rest there is a small gap *g* provided between the actuator and the tube. This gap was designed for the ease of inserting the Parylene tube into the DRIE pump structure during the assembly process.

The value of this gap g is kept as 5 μm. There is also another gap g_1 provided between the top of actuators and the base of the Parylene side handle. This gap is provided with the help of bonding material between the top glass plate and the SOI wafer. The value of g_1 is around 10 μm. The dimension of the area of the electrothermal actuator, which will be in contact with the Parylene tube, is 750 μm × 100 μm and the area of the actuator that will actually come in contact with the tube is 750 μm × 90 μm. This is because of the gap g_1 provided and the geometry of the tube. This area will contact with the tube symmetrically at the center. The area of the tube that is in contact with the actuator is shown in Figure 4.4. The Parylene top cover is bonded to the U shape Parylene structure and also is attached to its glass substrate. In this way the whole tube structure is attached to the top glass cover and is suspended into the DRIE pump die as shown in Figure 3.3.

Mechanical structure of the Parylene tube analyzed done using ANSYS 9.0. Certain assumptions were made while doing the analysis. The walls of the tube were assumed to be plates. So the theory of plates can be applied to the wall deformation. But due to the complex boundary conditions of the walls, an analytical solution was not possible in this case. HYPERELASTIC SOLID186 also called, SOLID186 was the element type used for modeling the tube structure in ANSYS. SOLID186 is a higher order 3-D 20-node structural solid element. SOLID186 has quadratic displacement behavior. The element is defined by 20 nodes having three degrees of freedom per node: translations in the nodal x, y, and z directions. SOLID186 may have any spatial orientation. The element supports plasticity, hyperelasticity, creep, stress stiffening,

large deflection, and large strain capabilities. It also has mixed formulation capability for simulating deformations of nearly incompressible elastoplastic materials, and fully incompressible hyperelastic materials [41]. The material properties that are required for the modeling and simulation i.e. Young's Modulus, Poisson's Ratio and Density is taken from the Table 4.1. The model is generated in ANSYS and is meshed using 'smart mesh' option. Due to the symmetry of the structure, only 18^{th} of the structure was modeled. The tube model is shown in Figure 4.3.

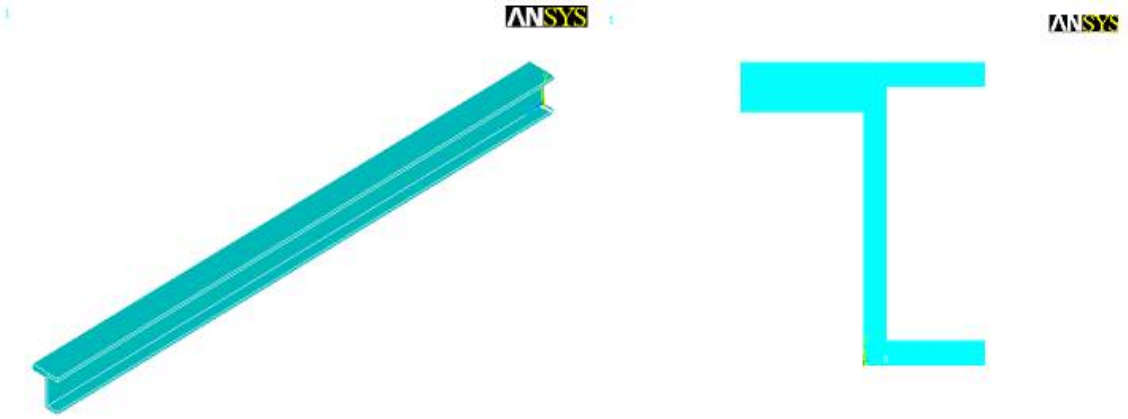

(a) (b)

Figure 4.3 ANSYS Model for tube thickness of 10 μm (a) Half Parylene tube, (b) Cross-section of the half Parylene tube.

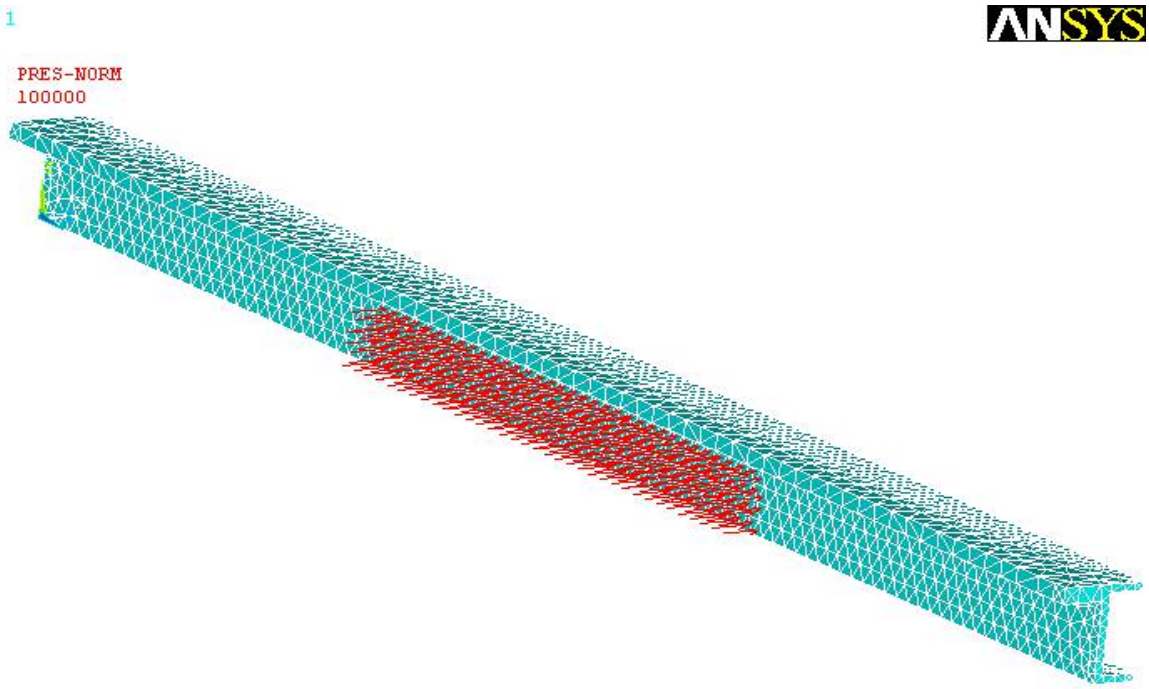

(a)

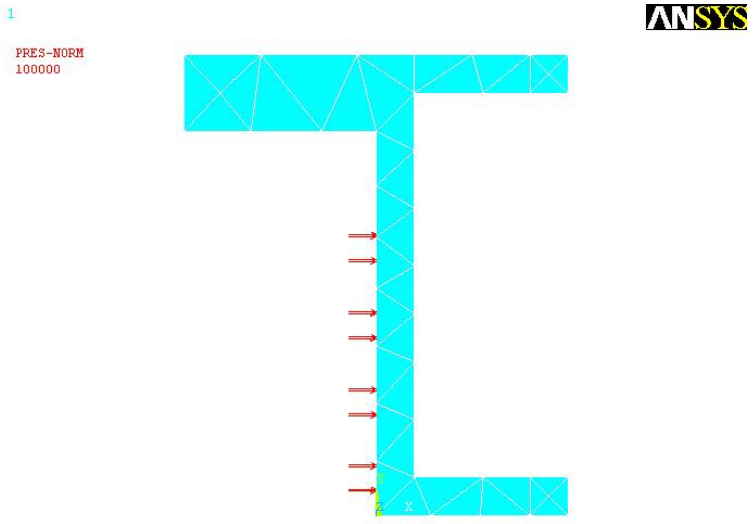

(b)

Figure 4.4 ANSYS Model for tube thickness of 10 μm (a) Elements of the half Parylene tube showing the region where the pressure is applied, (b) Cross-section of the half Parylene tube showing the region where the pressure is applied.

The problem was solved in ANSYS and the results were obtained for value of pressure ranging from 100 kPa to 120 kPa and the value of thickness t of the tube ranging from 10 μm to 4 μm. Figure 4.5 shows the nodal solution for displacement sum vector and Figure 4.6 shows the von-Mises stress distribution within the tube structure. Figure 4.7 is the plot of maximum deformation with applied pressure and different wall thickness. Figure 4.8 is the plot of the maximum von-Mises stress with applied pressure and different wall thickness.

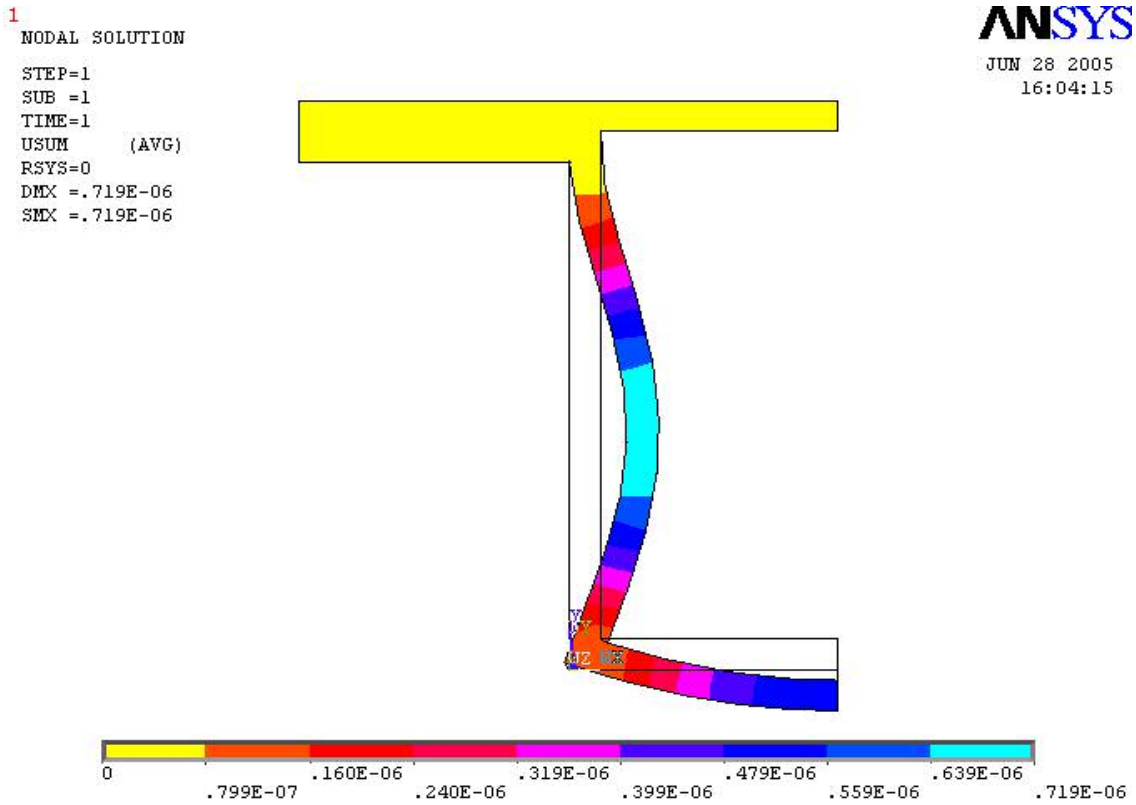

Figure 4.5 Nodal solution for displacement sum vector at thickness of 6 μm and applied pressure of 100000 Pa, showing the maximum displacement near the middle of the sidewall.

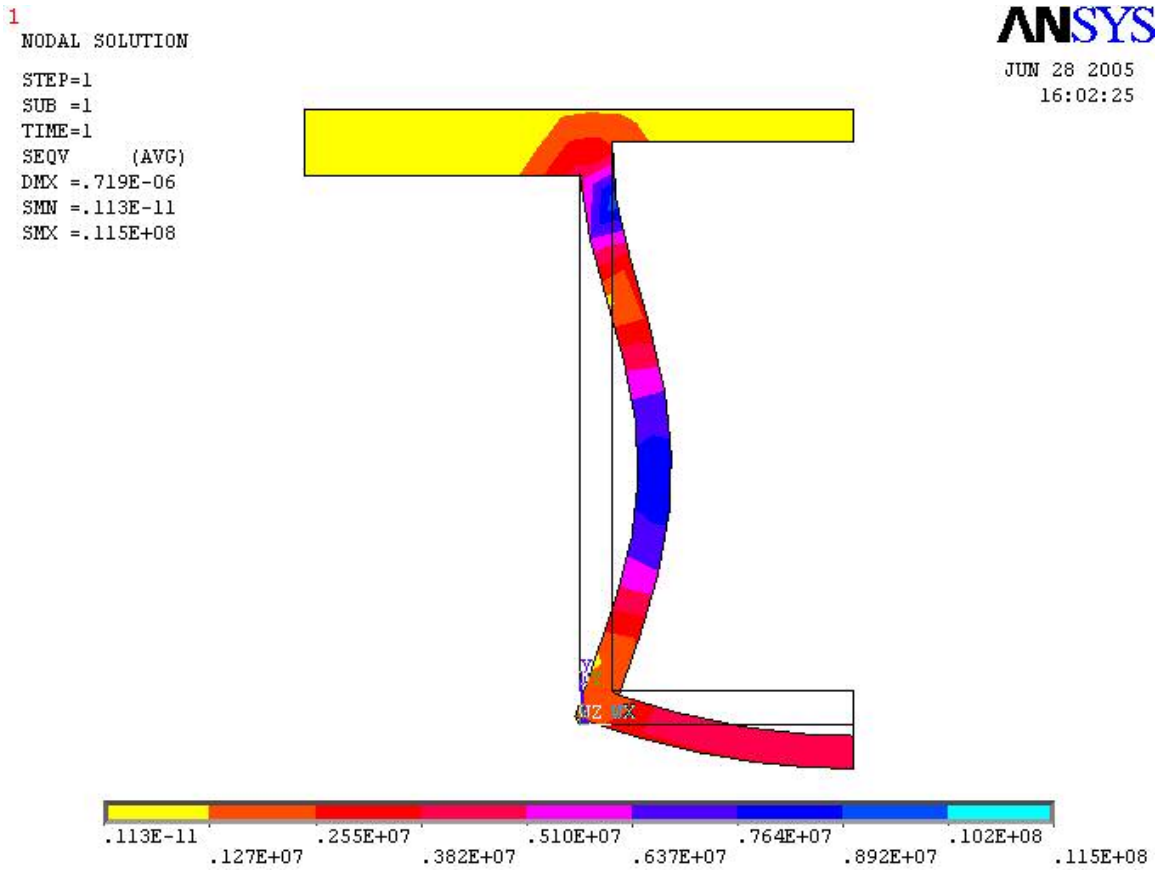

Figure 4.6 Nodal solution for von- Mises stress distribution at thickness of 6 μm and applied pressure of 100000 Pa, showing the maximum stress near the middle and the upper corner of the sidewall.

The results show that the maximum deformation is achieved at the middle of the sidewall. It is observed that the maximum deformation is achieved for the minimum thickness of the tube analyzed i.e. 4 μm. Also it is observed that the von-Mises stress increases with decrease in thickness and pressure applied. As expected, the maximum value of the stress is at the top corner of the tube. This is due to the sharp corner and the boundary conditions applied. The top surface of the tube is attached to the glass cover and so it has no motion.

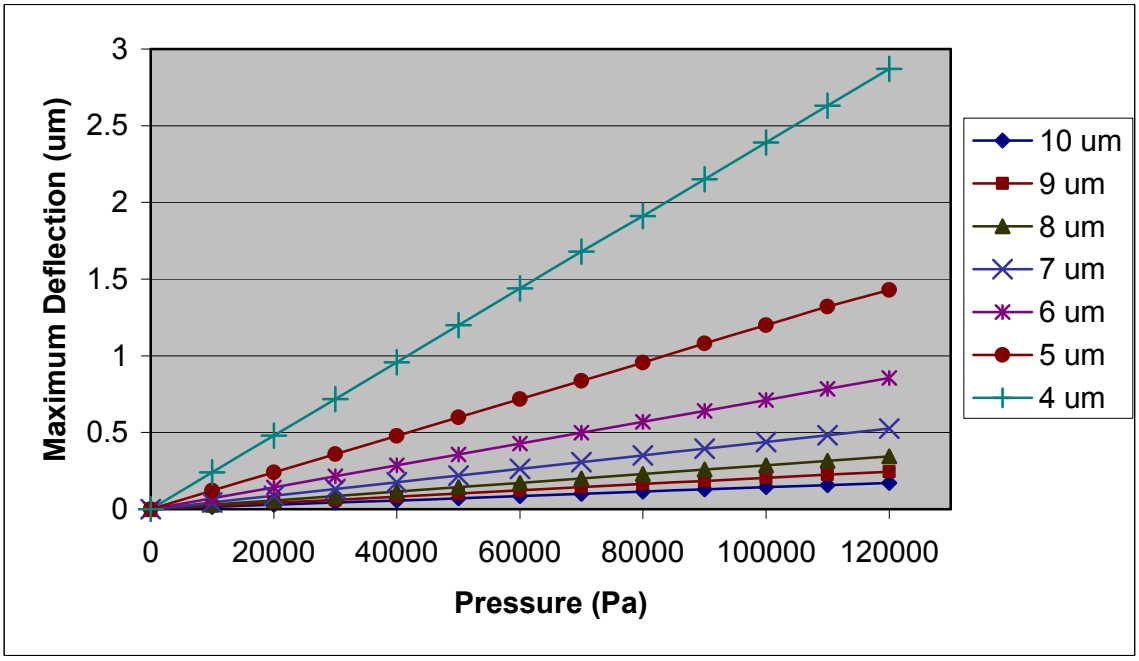

Figure 4.7 Graph of change in maximum deformation with applied pressure for different wall thickness.

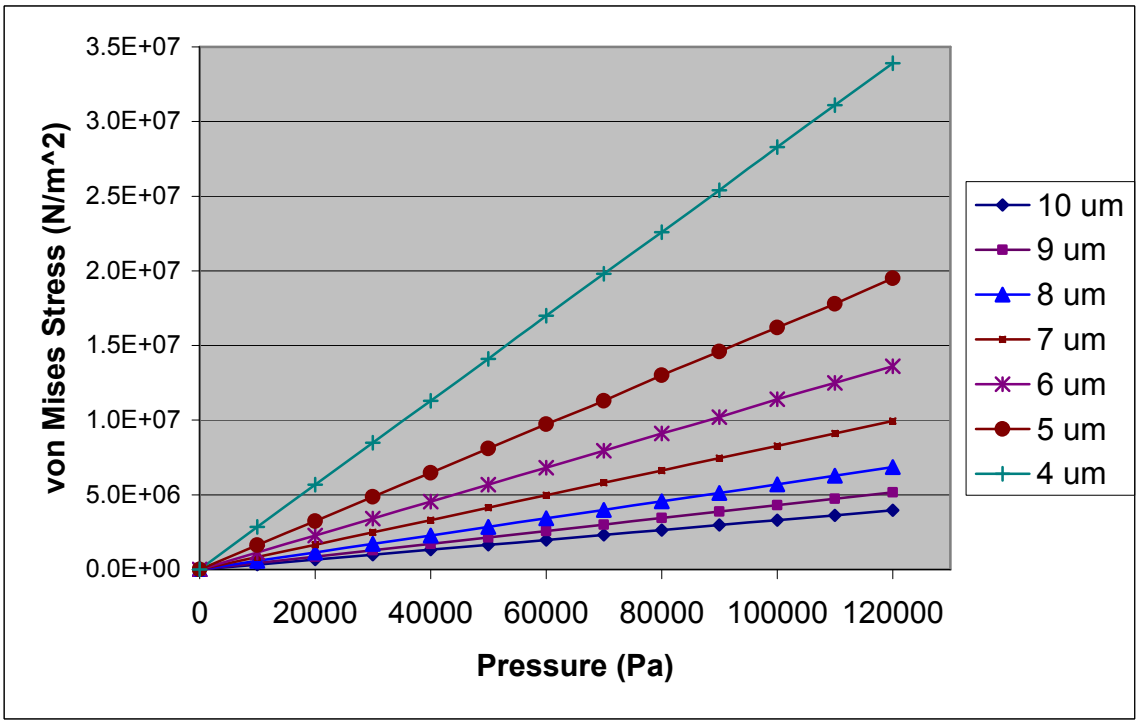

Figure 4.8 Graph of change in von-Mises stress with applied pressure for different wall thickness.

The deflection results show that even for a 4 μm thick tube and an applied pressure of around 100 kPa, the deflection is small. This small deflection gives a small stroke volume. The flow rate of the pump is directly proportional to the stroke volume [25], therefore a different geometry of the Parylene tube was designed. This design had an aspect ratio greater than 1:1. It took the advantage of the present fabrication process, which can easily manufacture Parylene tube of greater aspect ratios. The new cross section dimensions of the tube were 50 μm × 150 μm × 1000 μm (width × height × length). The similar analysis was performed on this design. The deflection results are shown in Figure 4.9 and the stress results are shown in Figure 4.10. The analysis was performed for tube thicknesses ranging from 4 μm to 10 μm for an applied load of 100 kPa. One disadvantage of the new design was that the height was greater than the height of the device layer of the SOI wafer, which is 100 μm.

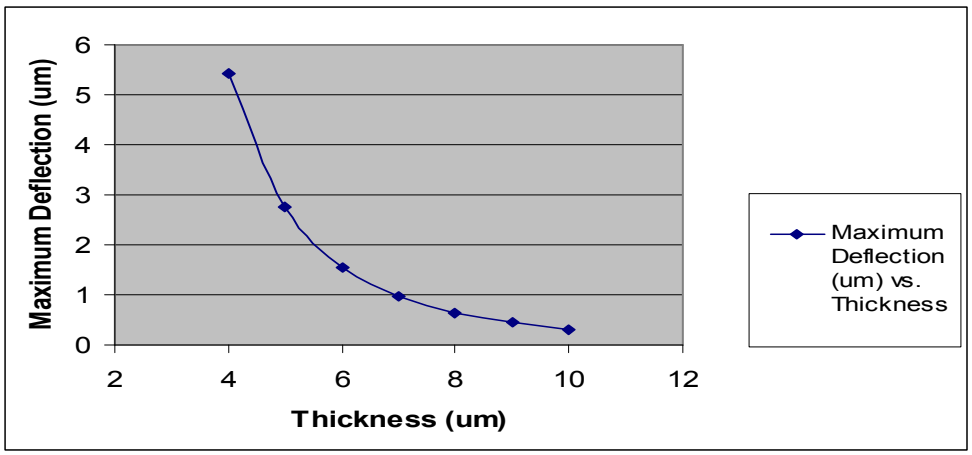

Figure 4.9 Deflection results showing maximum deflection for different tube thickness and for an applied pressure of 100 kPa.

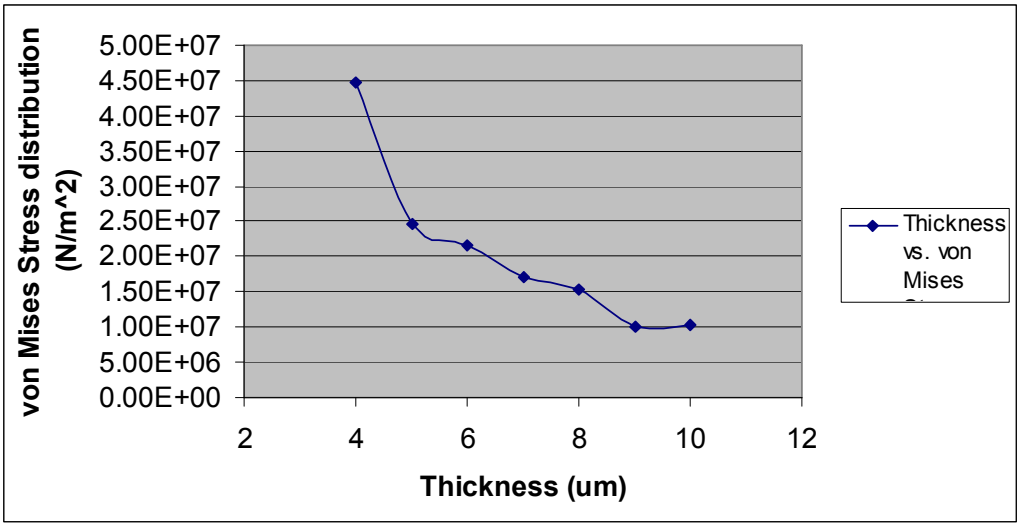

Figure 4.10 Stress results showing von-Mises stresses for different tube thickness and an applied pressure of 100 kPa.

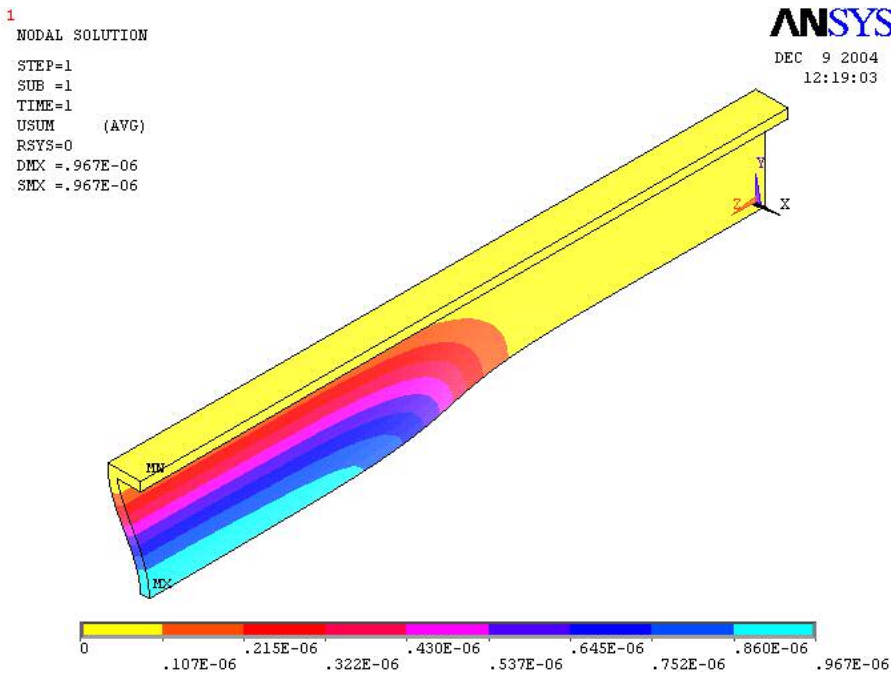

Figure 4.11 ANSYS result showing deflection for a 7 μm thick Parylene tube.

In order to accommodate the 150 μm height of the tube, an additional DRIE step was required in the fabrication process for the backside etch of the SIO wafer. The maximum deflection achieved for a 4 μm thick tube for 100 kPa was 5.42 μm.

4.2 Parylene tube design for maximum compression ratio

In most cases the compression ratio is the measure of the performance of the pump. It is the ratio of stroke volume to the dead volume. Stroke volume is also called the volumetric displacement. It is the volume displaced within the compression chamber when the external actuator actuates the pump diaphragm. The dead volume is the volume of fluid within the compression chamber when the diaphragm is at its normal position i.e. when the actuator does not actuate it.

Compression Ratio = Stroke Volume / Dead volume

$$\text{i.e. } \varepsilon = \frac{\Delta V}{V_0}$$

Where,

ε = Compression Ratio

ΔV = Stroke Volume

V_0 = Dead Volume

The stroke volume for a given pump is usually calculated analytically by applying the equation of plate deflection. This is usually done numerically by solving the governing equation, knowing the boundary conditions. Due to the complicated boundary conditions with this design, it was not possible to determine the boundary conditions analytically. Hence a unique method for the compression ratio calculation was employed in this study. The tube cross-section dimensions used for this analysis were 50 μm × 150 μm (Width × Height) and the tube length was taken as 1000 μm. The compression ratios were calculated for various thickness t of the tube ranging from 10

μm to 4 μm. The applied pressure was 100 kPa at the center of the tube. The area of the actuator, which contacts with the tube, was 750 μm × 100 μm.

Then the nodes of the internal face of the tube 1/8th model were selected. This process was followed by visually reselecting the nodes from the already selected nodes in order to form an array of nodes. There were eighteen columns and six rows of nodes selected. The selection and reselection of these nodes is as shown in Figure 4.12.

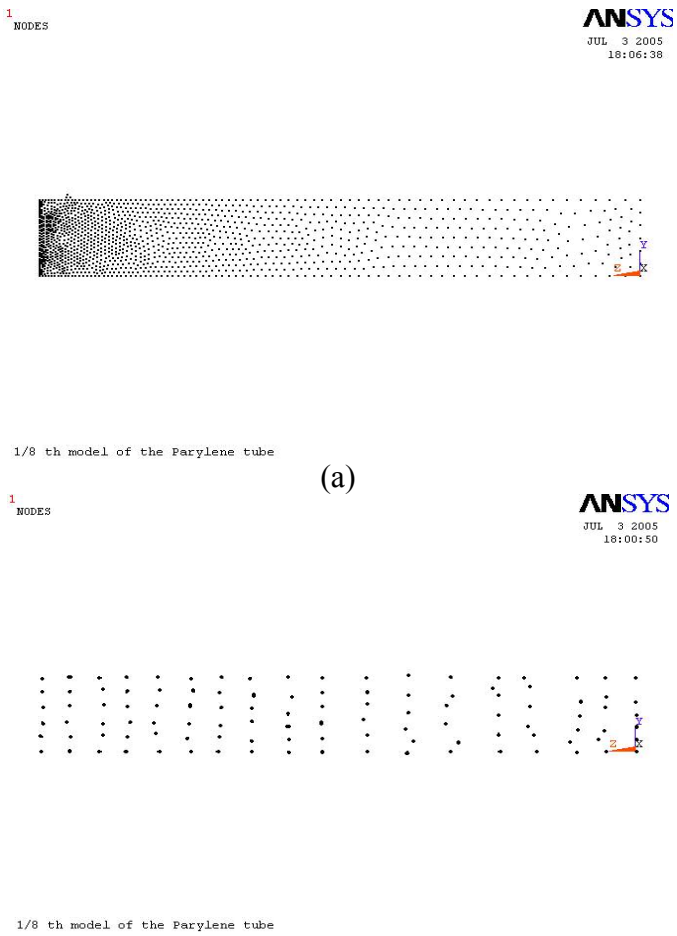

Figure 4.12 (a) Nodes of the internal face of the 1/8th tube model. (b) Reselected nodes on the internal face so as to form an array of 6 × 18 nodes for 3D profile plotting.

The Y - coordinates of the nodes in each row were averaged to get one value of Y – coordinate for nodes in that row. Similarly the X – coordinates of nodes in each column were averaged to get one value for the X – coordinates for the nodes in that column. So now we get six values for Y – coordinates and eighteen values for X – coordinates. In this way we form an array of 6 × 18 nodes. Now the deformation results in X direction i.e. UX were noted for all these selected nodes as X direction was the direction of actuation. The UY and UZ deformation components were neglected, as these values were negligible as compared to the X direction deformation values. These values along with the respective X and Y coordinates were noted and were plotted into MATLAB. The resulting 3D plot gave an approximate profile of the deflected internal face of the $1/8^{th}$ tube. The Figure 4.13 shows the deformation profile generated in MATLAB.

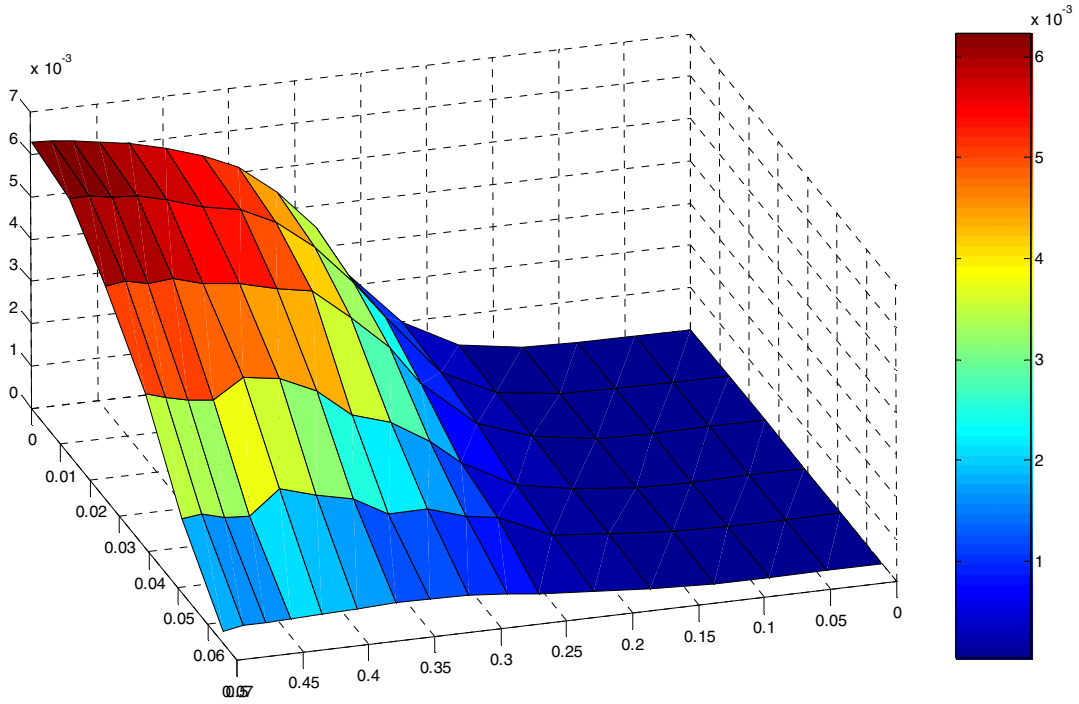

Figure 4.13 3D plot of the deflected internal face of the 1/8th tube generated in MATLAB. All dimensions in mm.

The volume below this 3D plot is the swept volume. To calculate this swept volume, this 3D surface profile was approximated to the 3rd order polynomial and it is triple integrated. This will give the volume below the surface. This surface profile for 3rd order approximation is shown in Figure 4.14.

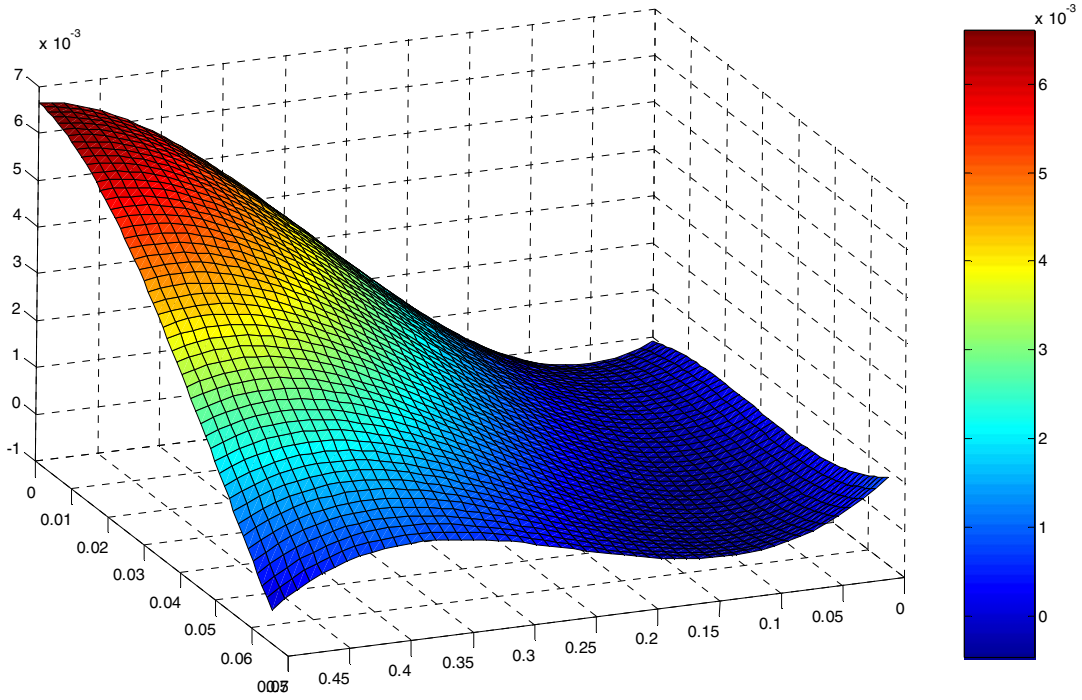

Figure 4.14 3rd order approximation of the deflected internal face of the 1/8th tube generated in MATLAB. All dimensions in mm.

Multiplying this volume by eight will give the total swept volume in the pump chamber. In this way the compression ratio was calculated for tubes of thickness t ranging from 10 μm to 4 μm for an applied pressure value of 100 kPa. The Figure 4.15 shows the trend in the variation of the compression ratio with respect to the thickness of the tube. As expected, the compression ratio goes on increasing as the tube thickness goes on decreasing. This is because the deformation goes on increasing with decrease in the tube thickness.

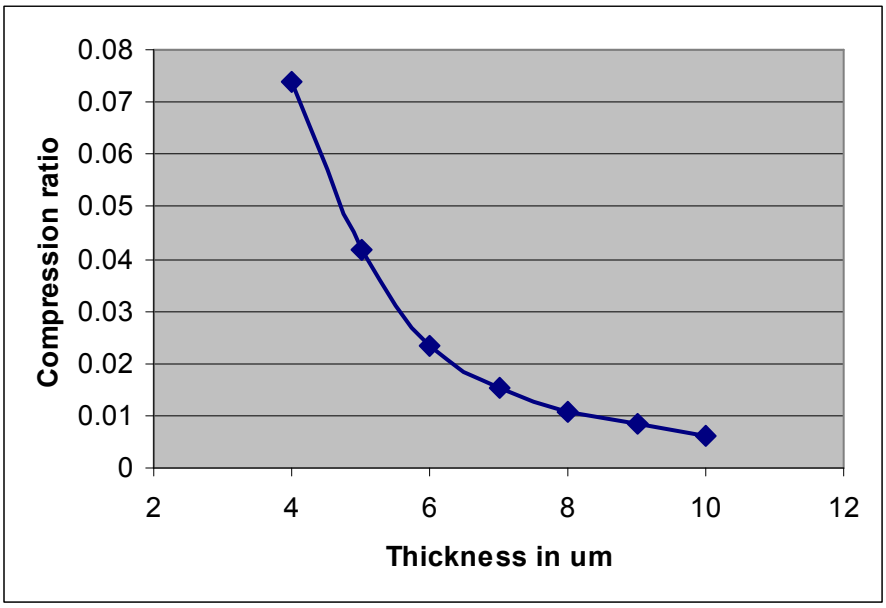

Figure 4.15 Compression ratio calculated at various tube thicknesses (t) at applied pressure of 100 kPa.

4.3 Quasi static modeling of the Parylene tube

The actuator is operated is in the operating frequency range of 50 Hz to 100 Hz. This is the same frequency at which the Parylene tube will be oscillated or excited. At such lower operating frequencies, the dynamic behavior of the tube can be neglected. So we can neglect the inertia of the membrane and the acceleration of the fluid in contact with the tube internal surface. In short, the inertia effects are neglected, i.e. the input can be transient but the response is steady state. This is the quasi-static model assumption. The pressure distribution within the chamber is spatially uniform, i.e. local fluid redistribution inside the pumping chamber occurs quasi-statically, that is, instantaneously on the time scale considered [43]. The lower operating frequencies are sufficient assumption for the quasi-static consideration. The quasi-static behavior is not valid for higher operating frequencies such as above 300 Hz and above [5]. If the

natural frequency value of the Parylene tube, with considering fluid inside it, is of the order of 10 greater than the maximum frequency of the quasi-static simulation then the quasi-static assumption is valid and therefore no interference with the dynamic behavior can be expected [5]. The whole purpose of the following study is to validate that the dynamic behavior can be neglected, i.e. to prove the quasi-static assumption to be valid.

Modal analysis is done to find out the natural frequencies of the Parylene tube. Usually the natural frequencies are found by neglecting the effect of the surrounding medium on the structural vibrations. The effect of the surrounding fluid on the natural frequency and mode shapes of a structure is not ordinarily significant for relatively compact structures if the fluid density is much dense than the average density of the structure [44]. Thus the surrounding air will not ordinarily affect the natural frequencies or mode shapes of most metallic structures. However, if the surrounding medium is a liquid, and if the solid structure has a relatively low density, the effect of the surrounding fluid over the natural frequency of the structure will be significant [5, 43, 44].

In microfluidics, the structural components operate in liquids with high viscosity. Therefore, damping occurs which decreases the resonance frequency. This effect can be mathematically described with an 'added' mass m_a [5, 44]. m_a is a generally a function of the geometry, boundary conditions and mode number [43]. The natural frequency of an elastic structure is inversely proportional to the square root of its mass. The effect of this added mass on the natural frequency can be expressed as

$$v_i(fluid) = \left(1 + \frac{m_a}{m_o}\right)^{-0.5} v_i(vacuum)$$

Where,

m_o = original mass of the structure,

m_a = added mass

v_i (vacuum) = natural frequency of the structure in vacuum

v_i (fluid) = natural frequency of the structure surrounded by fluid

ANSYS 9.0 is used find out the natural frequencies of the Parylene tube structure. The values of natural frequencies of the tube surrounded by vacuum were found out for different tube thickness. The thickness values ranged from 4 μm to 10 μm. These values are tabulated in Table 4.2. The other dimensions of the tube were 50 μm × 150 μm (Width × Height) and the tube length was taken as 1000 μm. The ends of the tube and the top portion of the tube were fixed. Symmetry of the tube structure was utilized for ANSYS simulation purpose.

Table 4.2 First natural frequency of the Parylene tube surrounded by vacuum with different thickness.

Thickness (μm)	First Natural Frequency (Hz)
4	15113
5	18348
6	21788
7	23963
8	27828
9	30891
10	32552

To consider the effect of fluid on one side of the tube, the fluid was considered as an added mass, which caused damping of the vibrations. For the simplicity of this analysis, the tube portion, which was actuated by the actuator, was considered as a rectangular plate. For a rectangular plate with one side exposed to fluid, the following expression for added mass was suggested by Greenspon [44, 45]

$$m_a = \alpha_{ij} \beta \rho a b^2$$

Where,

$$\alpha_{ij} = \frac{\left(\int_A \tilde{z}_{ij} dA \right)^2}{2ab \int_A \tilde{z}_{ij}^{\,2} dA}$$

Where $\tilde{z}_{ij}$ is the dimensionless mode shape of the *ij* mode. And *dA* is an element of the plate area $A = ab$, where *a* is the width of the plate and *b* is the length of the plate ($b \geq a$) and β is an aspect ratio dependent factor. The values of β and α_{ij} can be found out form [44] for the given values of *a* and *b*. This will give the value of the added mass m_a. This value of added mass was found out for tubes of thickness ranging from 4 μm to 10 μm and is tabulated in the Table 4.3. The Figure 4.16 shows the graph of natural frequency with and without considering fluid on one side of the tube.

From Figure 4.17 it can be concluded that the natural frequency values of the Parylene tube, even after considering fluid on one side, is to the order of 10 larger than the maximum frequency for quasi-static assumption. Thus the quasi-static assumption is valid and there is no need to consider the dynamic effect.

Table 4.3 First natural frequency of the Parylene tube surrounded by fluid on one side with different thickness.

Thickness (μm)	First Natural Frequency (Hz)
4	3528
5	4780
6	6226
7	7362
8	9168
9	10709
10	11887

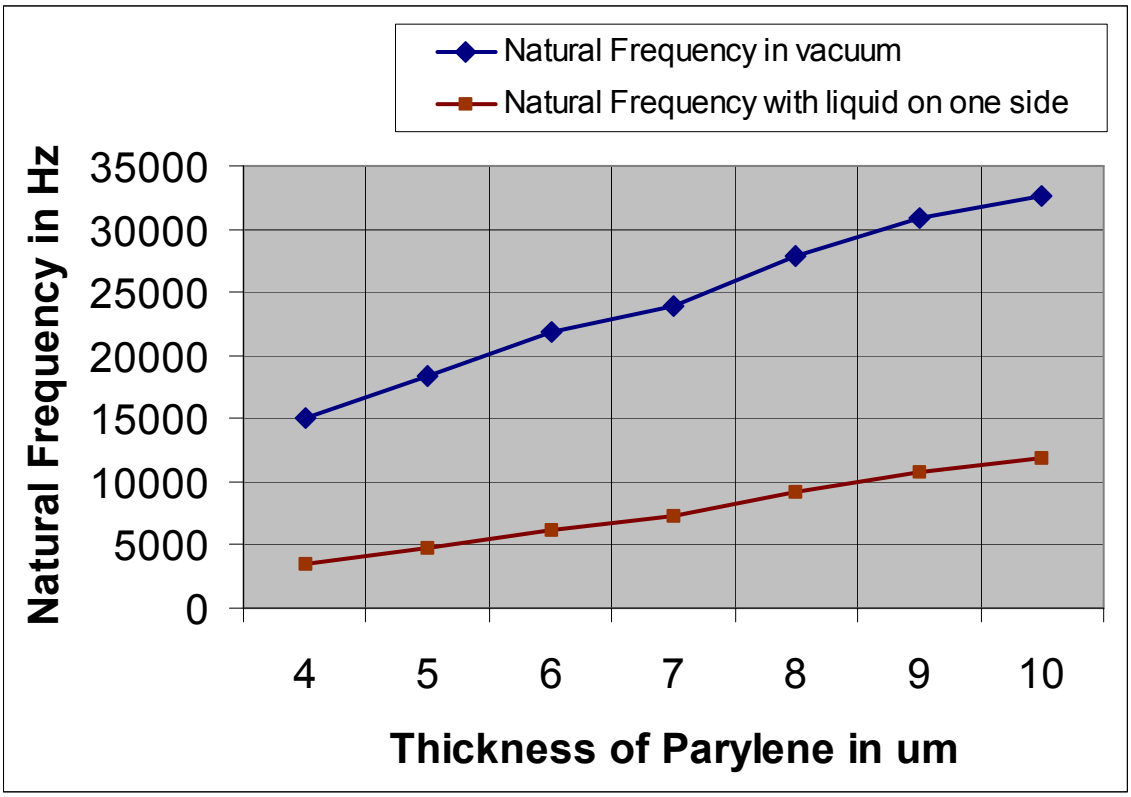

Figure 4.16 First natural frequency of the Parylene tube with and without considering the effect of fluid on one side.

4.4 Analysis and simulation of the thermal actuator

Electrothermal actuation principle is utilized in the present study to actuate the Parylene tube. Two electrothermal actuators are placed on the either side of the Parylene tube in such a way that there is a 5 μm gap between the tube and each actuator when the actuators are not excited. The actuator consists of two pads for electrical contact, the V beams and the part, which comes in contact with the Parylene diaphragm. When electrical voltage is applied to the actuator, the force caused by the rib's expansion pulls or pushes a rigid bar that is pivoted by a thin flexible bar. This is called the electrothermal expansion principle. The electrothermal expansion provides higher

force compared to electrostatic methods. The magnitude of diaphragm deflection affects the intake volume and the compression ratio. It also in turn depends upon the applied voltage. Thus the pump flow rate is the function of the applied voltage. A typical electrothermal actuator with all its parts is shown in figure 4.17.

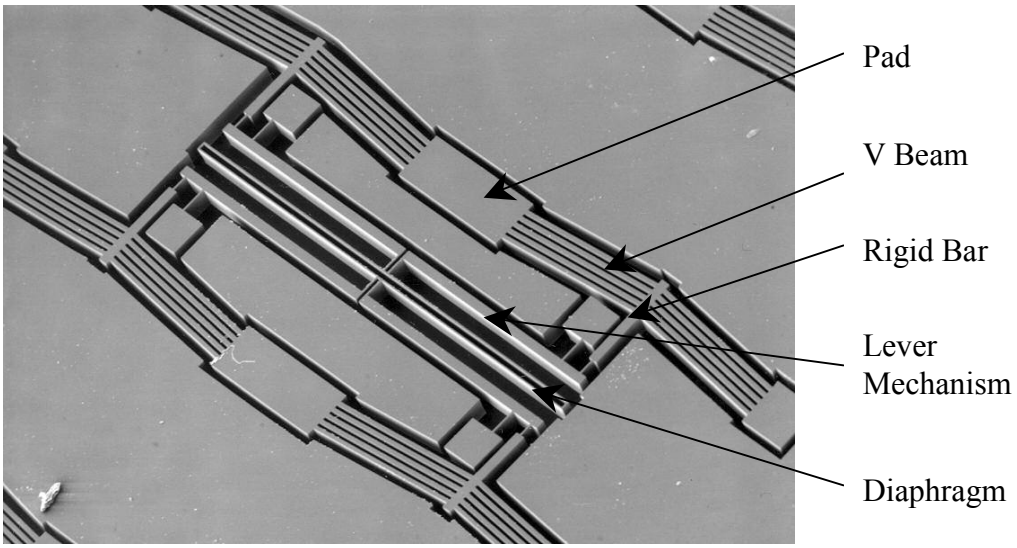

Figure 4.17 DRIE structure of the electrothermal actuator with all the components [17].

Stroke amplification mechanism was employed in [17] to get larger deflection of diaphragm. A lever structure was used for amplification purpose. The actuator is embedded into the pump structure. Modeling and simulation and optimization of the electrothermal actuator were reported in [17]. The actuator dimensions were 12 (width) × 100 (height) × 1200 (length) μm^3 and the rib angle was 5.7°. The power consumption was 2 W and the observed deflection was 30 μm at 12 V. It was observed that as the voltage goes on increasing, the silicon starts to melt due to high temperature and thus the rate of increase of deflection decreases. The goal of optimization was to reduce the driving power while achieving the desired pumping stroke and force [17]. MATLAB

was used as an optimization tool. The results showed that a larger value of the rib angle of 15° made the actuator stiffer so that it could withstand the reaction forces of the leaver mechanism. The driving power was optimized to 1 W. Thus the study showed that the pump driving power could be reduced with structural modifications. This study was for the initial design of the micropump, which did not utilize the polymer tube structure.

For the modified design of the micropump where the polymer tube is used the actuator design is also changed to suit the new design. The electrical contact pads, the V-beam ribs, the lever mechanism remains the same as the earlier design. The modification is done at the end where actuator comes in contact with the polymer tube. The actuator ends up in a flattened face, which will come in contact with the flat surface of the Parylene tube. In the earlier design this region was attached to the diaphragm, which directly came in contact with the fluid. The modification in the design enables to avoid the direct contact of the electrothermal actuator with the pumped fluid. The modified design is shown in Figure 4.18.

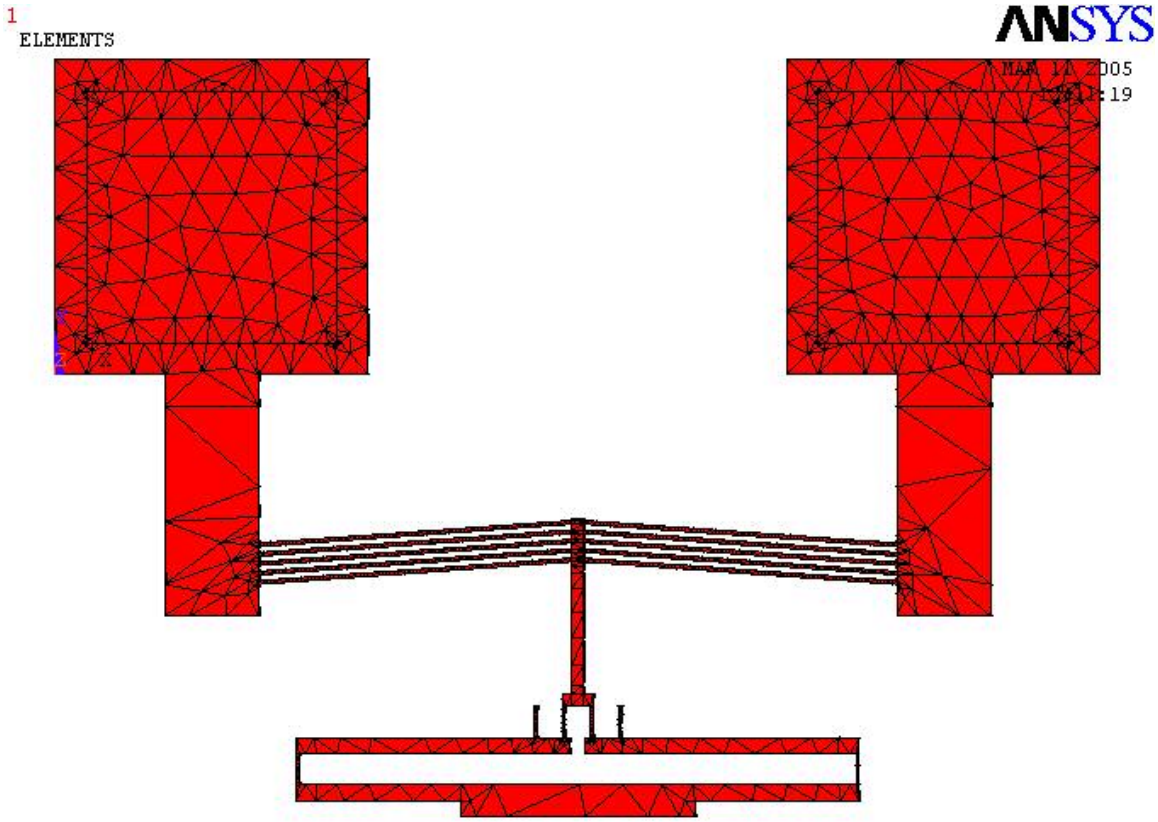

Figure 4.18 Modified design of the electrothermal actuator generated in ANSYS 9.0.

The new actuator was of dimension 10 (width) × 100 (height) × 1000 (length) μm^3. The rib angle is 3.43°. Initial analysis was done on this design to find out how the displacement and temperature behaves with change is applied voltage across the pads. ANSYS 9.0 was used for this purpose. The 3D model was generated in ANSYS 9.0. The element type used was SOLID98. SOLID98 is a 10-node tetrahedral element. The element has a quadratic displacement behavior and is well suited to model irregular meshes. This element type has default degrees of freedom as UX, UY, UZ, TEMP, VOLT and MAG. This element simulates the coupled thermal-electric-structural

response. The material properties used for the silicon in the finite element analysis of the electrothermal actuator are given in the Table 4.4.

Table 4.4 Material Properties of silicon in μMKSV units.

Material Properties of silicon in μMKSV units	
Young's Modulus	169×10^3 MPa
Poisson's Ratio	0.22
Resistivity	5×10^{-10} ohm-μm
Coefficient of thermal expansion	2.9×10^{-6}/°K
Thermal conductivity	150×10^6 pW/μm°K

The volume was smartmeshed with the coupled field elements. Then the voltage was applied to the electrical connection pads. Input voltage of 10 V to 15 V was applied to one pad and the other pad was grounded with 0 V applied over it. The temperature of the pads was fixed to 30 °C. The pads were mechanically fixed in X, Y and Z directions. The other required boundary conditions were applied and the problem was solved in ANSYS 9.0. Finally the solution was obtained and the result was post processed to achieve the analysis objectives. The results were obtained for values of voltage ranging from 10 V to 15 V and the Temperature-Voltage and the Displacement-Voltage relationship was observed. The displacement refers to the displacement at the region of the actuator, which comes in contact with the Parylene tube. Figure 4.19 shows the temperature distribution in the electrothermal actuator at the applied voltage of 14 V. Figure 4.20 shows the displacement in the Y direction of the electrothermal

actuator at the applied voltage of 14 V. Figure 4.21 and Figure 4.22 show the Temperature-Voltage and the Displacement-Voltage relationship respectively at the various applied voltages.

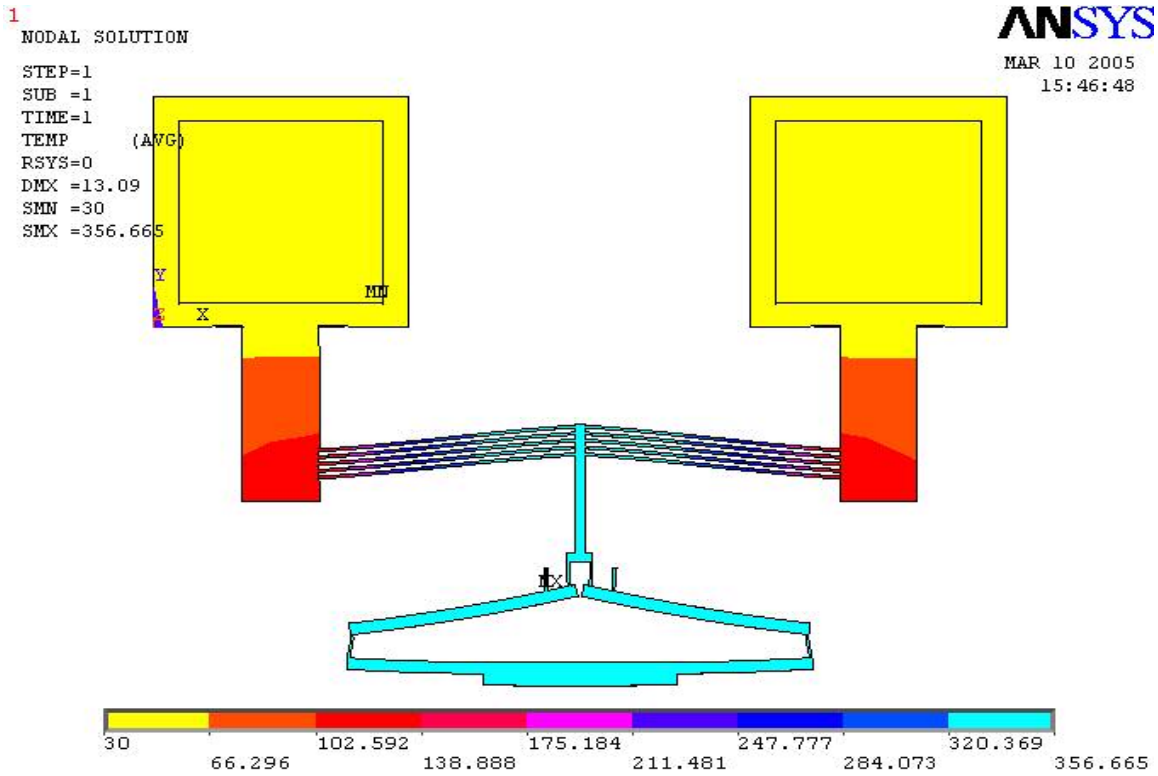

Figure 4.19 Temperature distribution in the electrothermal actuator at applied voltage of 14 V.

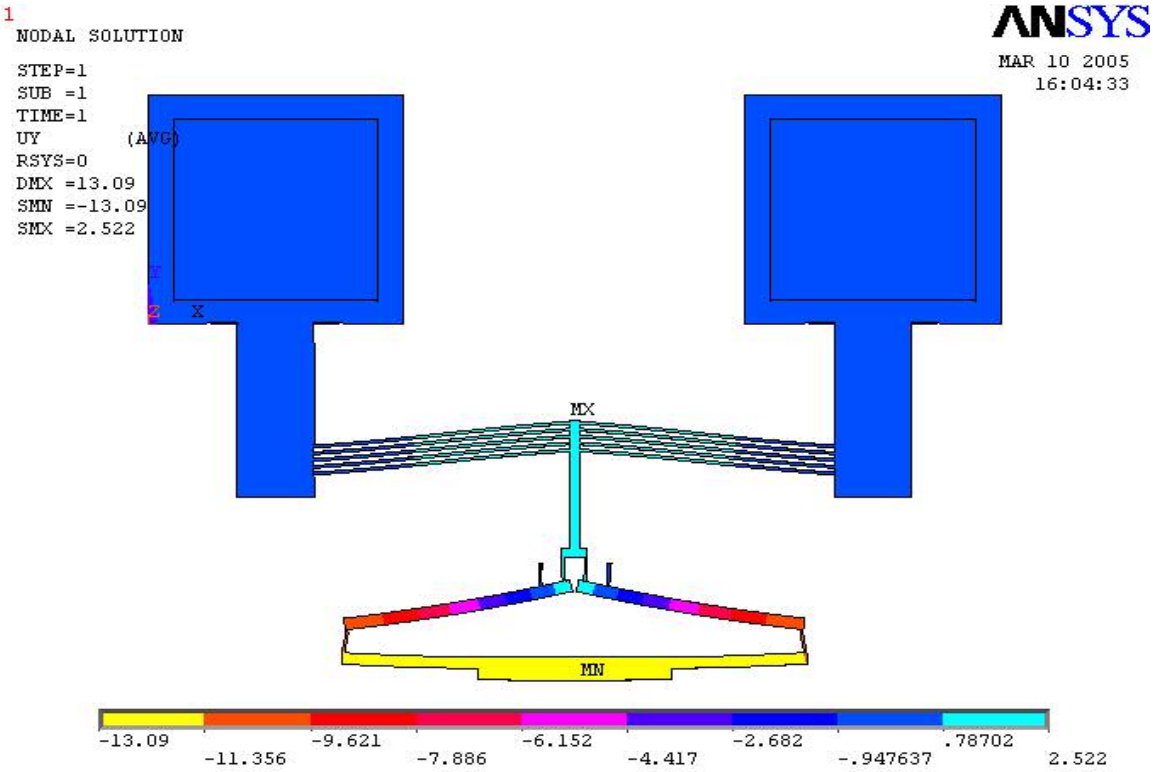

Figure 4.20 Displacement in the Y direction in the electrothermal actuator at the applied voltage of 14 V.

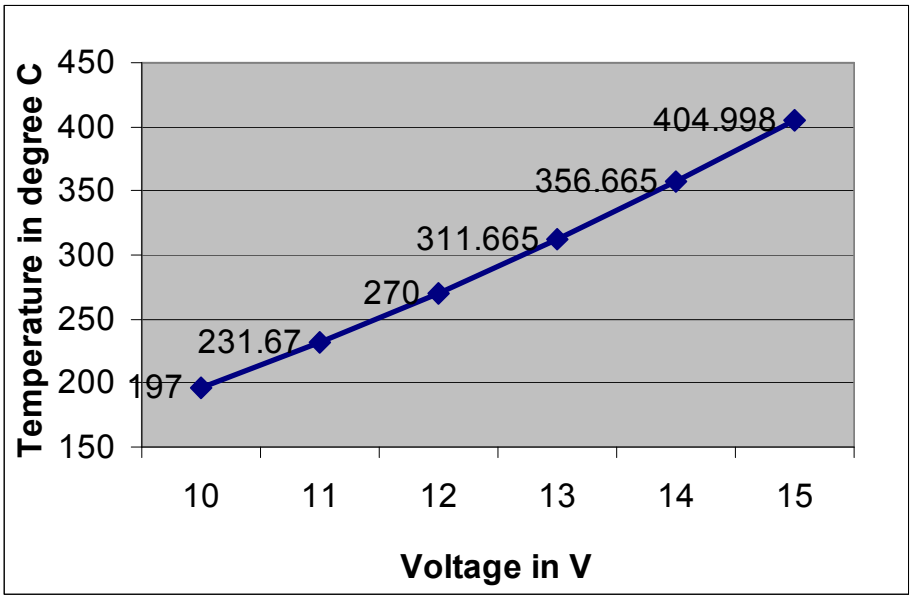

Figure 4.21 Temperature-Voltage at various values of the applied voltages.

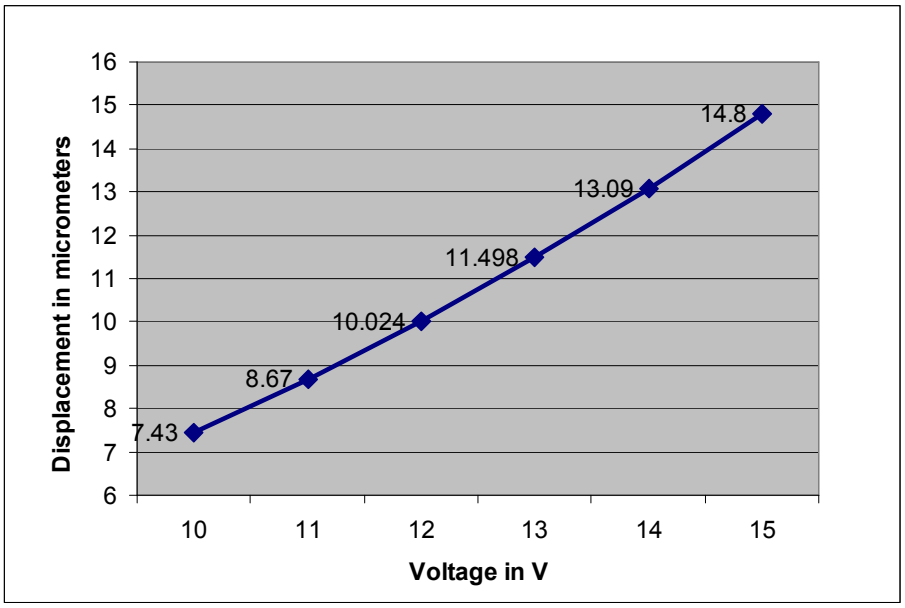

Figure 4.22 Displacement-Voltage at various values of the applied voltages.

The results show a linear relationship and a proportional increase in both the displacement and temperature with increase in voltage. It is observed from Figure 4.19 that the temperature at the end where the actuator will come in contact with the Parylene tube ranges from 320 °C to 356 °C. From Figure 4.21 it is found that the maximum temperature is achieved at 15 V and has a value of 404 °C. The expansion of the thermal V beam increases linearly with the input voltage. The joule-heating phenomenon takes place in the V beams. Although higher voltage is required to achieve larger displacements, the increase in temperature at the tube end limits input voltage. This is significant for the fact that the melting temperature of Parylene is 290 °C. The input voltage beyond 12 V can cause the Parylene temperatures higher than its melting temperature. With this constraint, the maximum displacement achieved was only 10 μm at 12 V input. To increase the displacement and the forces, the voltage needed to be

increased, and it should be possible without increase in the temperature at the tube. With the existing design of the electrothermal actuator this was not possible. Thus the existing design needed to be modified and optimized for maximum deflection and reduced temperature at the tube end of the actuator.

The whole purpose of the proposed design modification was to reduce the heat flow and thus the temperature increase at the tube while maintaining the high temperature at the V beams. Various modifications in the existing structure were suggested to suit the optimization purpose. Fins were introduced on the upper portion of the beams for the purpose of increasing the surface are for convection heat transfer. Also the volume for heat dissipation increased with addition of fins. The addition of fins provided a significant reduction in temperature. The dimensions of fins were selected arbitrarily and did not involves and shape optimization for maximum heat transfer purpose. The dimension of a fin was 150 (length) × 15 (width) and 100 (thickness) μm^3. The horizontal distance between the two fins was 25 μm. There were 17 fins provided on each end of the lever mechanism. The design modification is shown in Figure 4.23.

The electrothermal actuator was then modeled with the holes provided for etch release. This was not done in the initial simulation analysis. These holes are provided throughout the central rod and the lower beams. Addition of these holes reduces the temperature of the lower beam by about 10 °C. The flow of electricity and heat is directly proportional to the cross section area of the conducting material. The resistance in the current or heat flow increases with reduction in the cross sectional area. Thus lower current or heat will flow through the conductor of smaller cross section area. This

principle explains the reduction in the temperature after considering the holes in the modeling and analysis. The holes decrease the cross section area of the central rod and the lower beams. This causes a resistance in the current and heat flow. Thus less heat flows to the tube end of the actuator and thus the temperature at this end reduces. This design modification is shown in Figure 4.24.

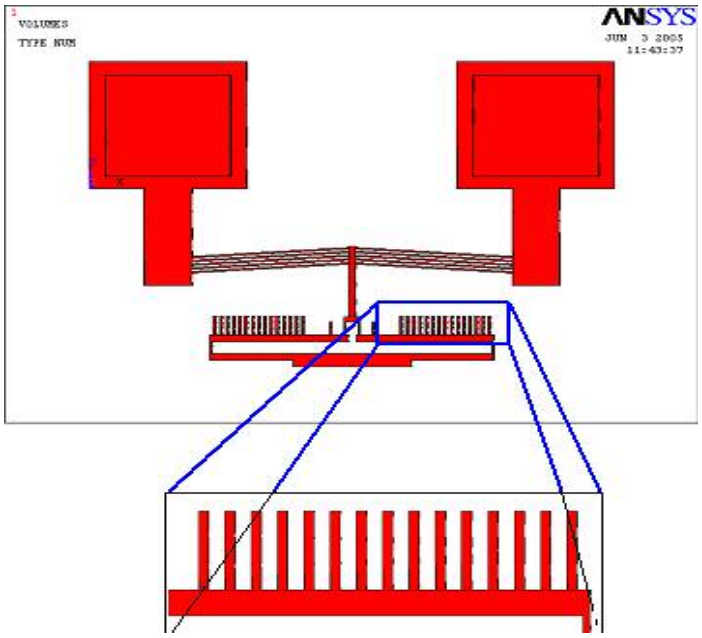

Figure 4.23 Electrothermal actuator modification by providing fins.

Another modification done to reduce the temperature at the tube end of the electrothermal actuator is the increase in the length of the central rod. This will increase the path length required for heat flow and thus less heat will flow downwards to the tube end of the actuator. Temperature reduction was about 10 °C with adding this feature.

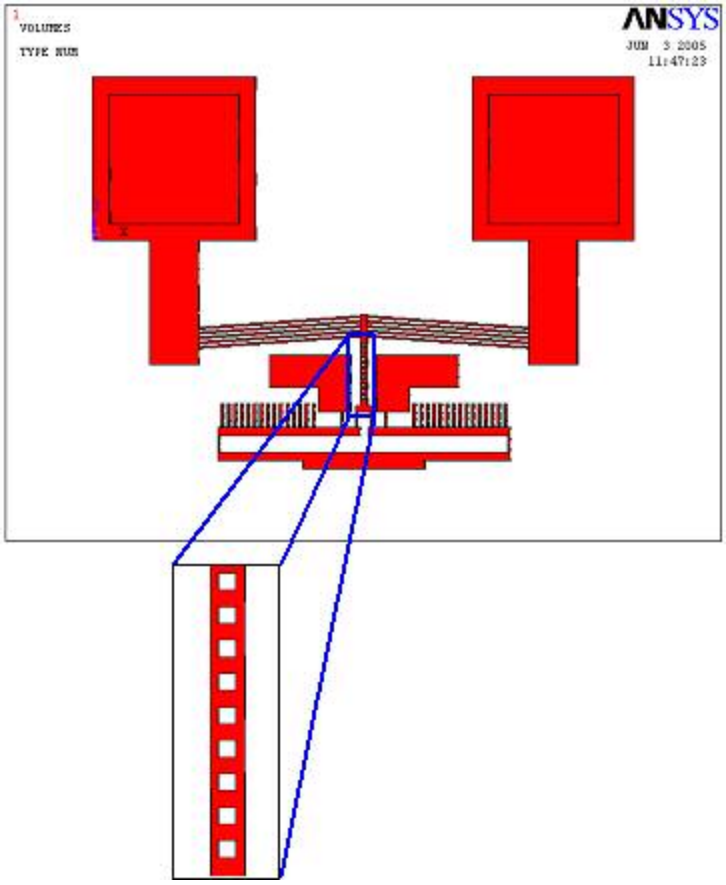

Figure 4.24 Electrothermal actuator modeling by taking the etch release holes into account.

The result of simulation due to the geometry change is summerized in Table 4.5. All the modification analysis was used input voltage of 15 V. This was aimed to ensure that the temperature at the tube end of the actuator is below the melting temperature of the Parylene even at the highest applied voltage. The temperature achieved at the tube end of the actuator was below the melting temperature of the Parylene tube by applying all suggested cooling features.

Table 4.5 Summary of the design modifications and its effect on the temperature and displacements at the applied voltage value of 15 V.

Design / Modification	**Temperature at the tube end of the actuator (°C)**	**Displacement of the tube end of the actuator (μm)**
Initial Design	404.98	14.81
After adding Fins	310.84	13.52
After adding holes in the rod	269.45	13.50
After increasing the length of the central rod	260.88	13.07
After adding holes and increasing the length of the rod by 450 μm	242.87	13.02

4.6 Various designs in LASI

Several new designs were generated based on the cooling features suggested. These designs were generated in a general purpose IC layout and design system called LASI (LAyout Systems for Individuals). These designs were then finally sent to fabricate the DRIE structure of the pump. The following figures will show the original design and the design with the cooling features. Each design shows two pumps designs on one 10 mm × 10 mm die. The essential parts are the pads for electrical connections, the V beam electrothermal actuators, the lever structure to transfer the motion of the V beam actuator to the Parylene tube, The diffuser / nozzle valves and the inlet and the outlet ports.

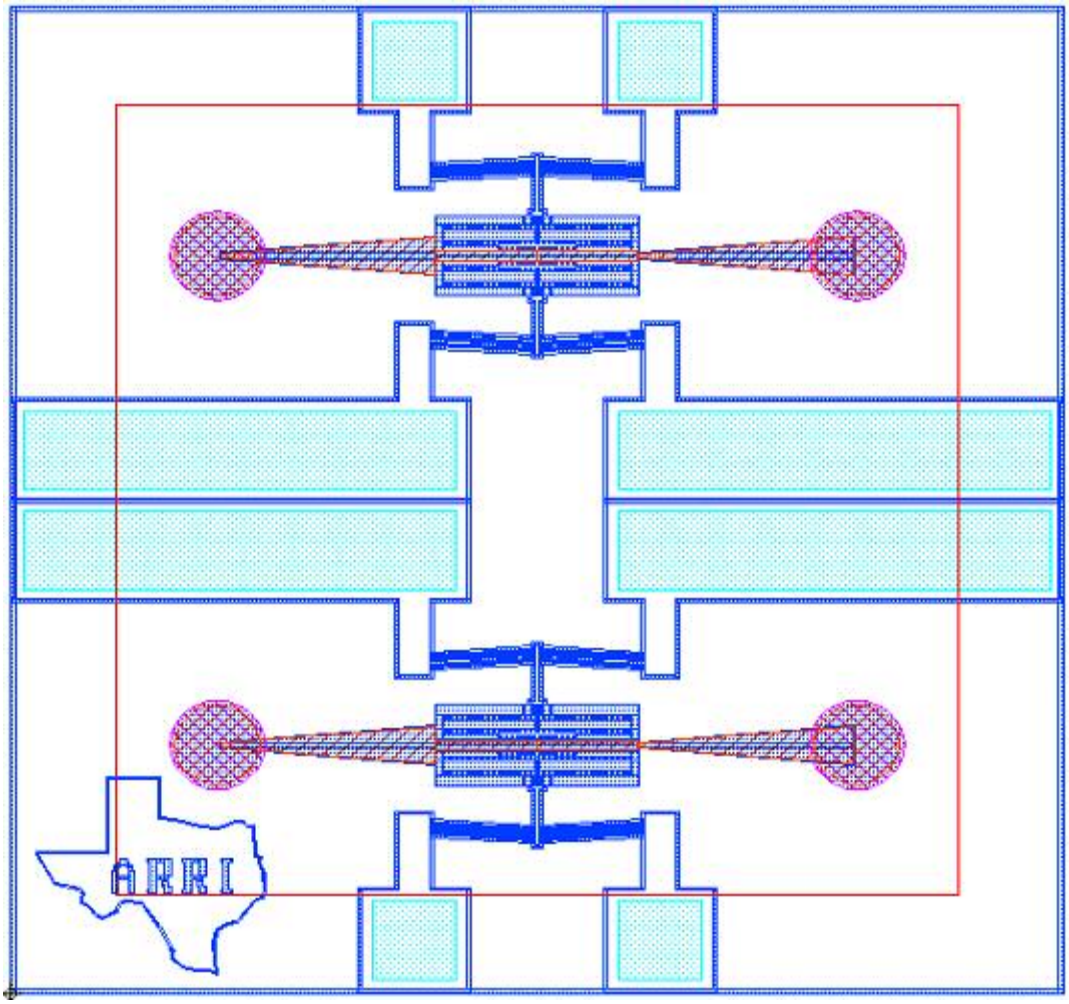

Figure 4.25 Initial design as interpreted in LASI.

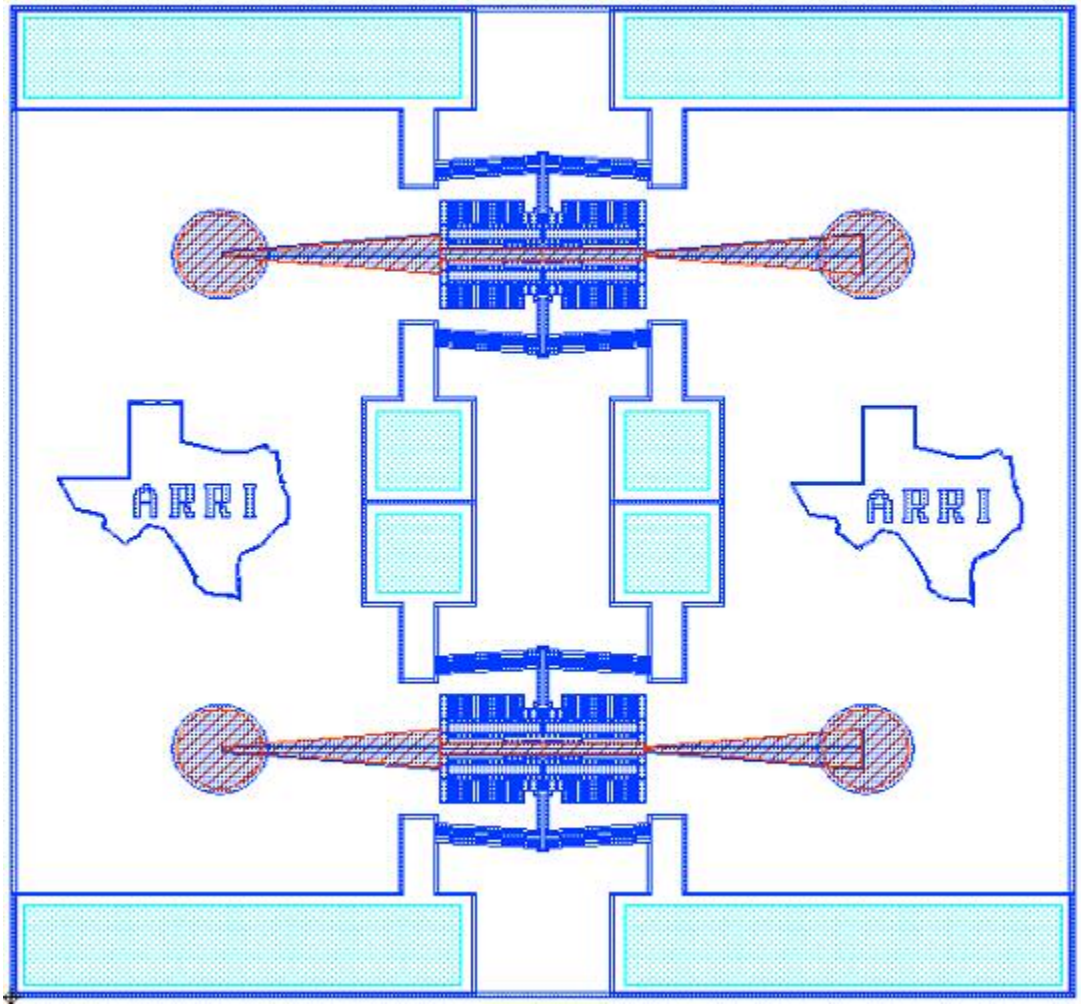

Figure 4.26 Design modified by adding fins.

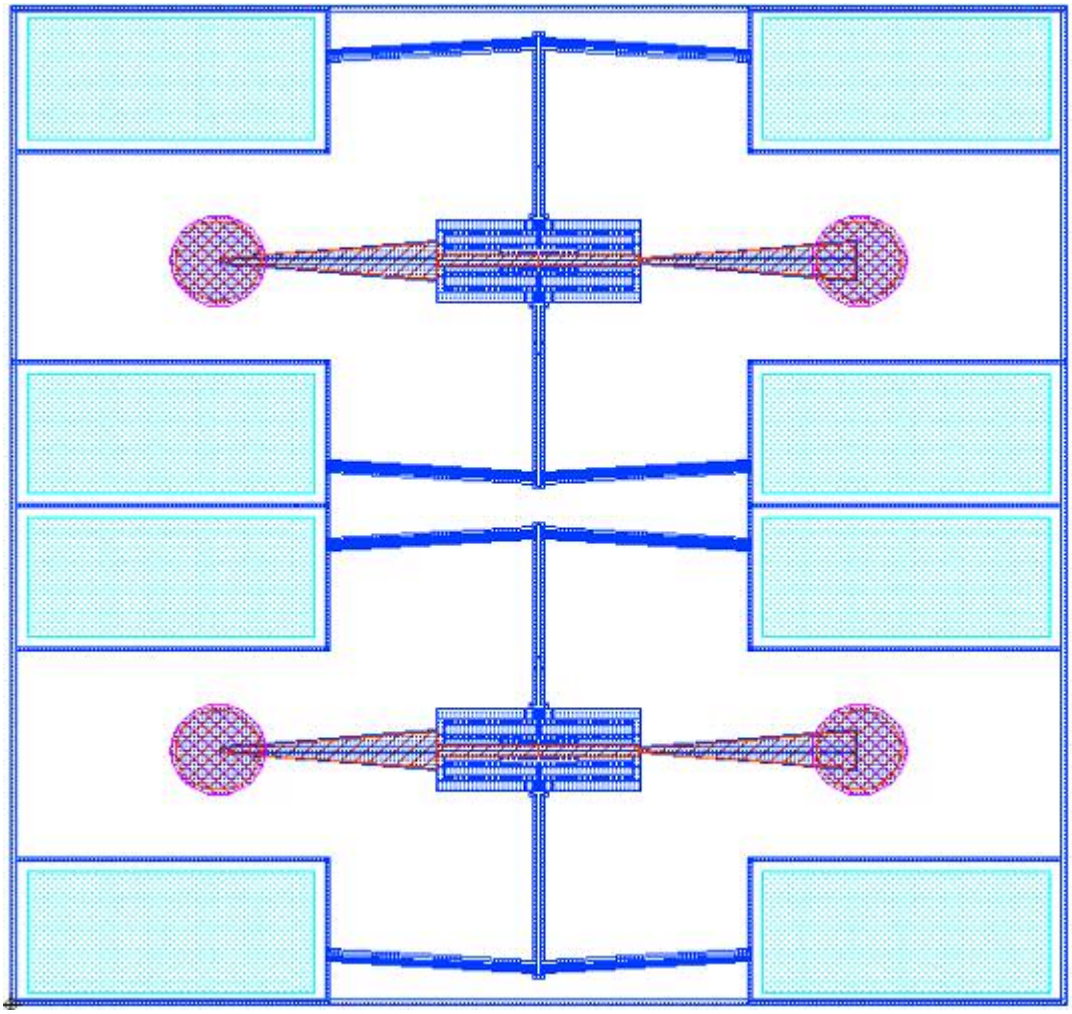

Figure 4.27 Design modified by increasing the length of the central rod.

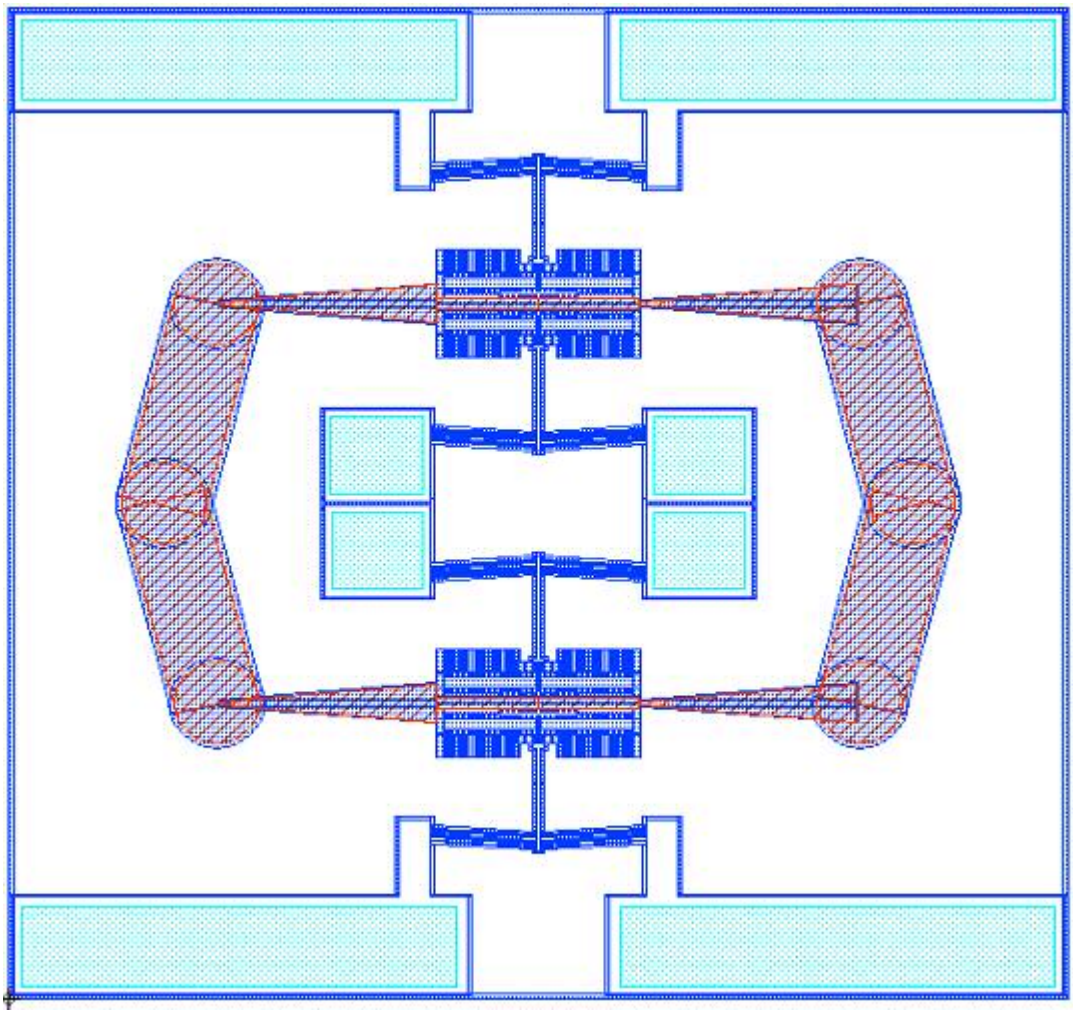

Figure 4.28 Continuous flow micropump design.

In the earlier designs the two pumps designed on a die were acting independent of each other. In that way, each pump produced an intermittent flow of fluid during a pump cycle. The fluid will be taken in into the compression chamber at the supply mode and will be delivered out at the pump mode. So there will be a pulse like flow at the outlet. This will create flow friction energy losses at the pump inlet and outlet [42]. These losses can be reduced in the double pump arrangement, where in the two pump chambers work anti-phase, therefore it reduces oscillation of the flow. The inlets and

the outlets of the pumps are connected together to form one common inlet and outlet. The pump capacity is also doubled as two pumps now act as one unit.

4.5 Characterization of the diffuser / nozzle valve structure

Diffuser / Nozzle value principle is used in the present study to direct the pumped fluid. This valve principle uses flow rectifying properties of the two nozzle / diffuser elements [42]. A diffuser is defined as a conduit with an expanding cross-section area in the flow direction and a nozzle is defined as a conduit with a decreasing cross-section area in the flow direction.

There exist a large number of different fluid pump principles. A conventional diaphragm consists of two passive check valves connected to an oscillating diaphragm, which creates an oscillating chamber volume [25]. When the chamber volume increases the inlet valve is open while the outlet valve is closed and the fluid flows through the inlet valve into the chamber (the supply mode). When the chamber volume decreases the inlet valve is closed and the outlet valve is open and the fluid flows through the outlet valve out of the chamber (the pump mode). The pumps with movable valves and other pumps with movable parts such as rotating pumps, may suffer from problems such as high pressure drop across the valves and the wear and fatigue of the movable parts. This may result in the reduction in the lifetime and reliability. There is also the risk that the valve action may cause damage to the sensitive fluids. These mechanical valves are also restricted to relatively low driving frequencies [31]. Other pumps with non moving parts such as electrohydrodynamic pump suffer from drawbacks that only polar fluids

can be used and low pump pressures are achieved even with very high driving voltages [25].

The pump presented here is based on the valveless pump principle, which uses different flow properties of a diffuser and a nozzle. The flow directing diffuser / nozzle element has no movable parts. There are two different types of behaviour for diffuser or nozzle structures. Depending on the angle of the truncated pyramid, the flow in the enlarging or the contracting direction is preferred. This difference in the preferred direction depends on the weight of each contributing factor [5]. For the larger opening angles like around 35°, the nozzle is the preferred direction of flow and the diffuser is the negative direction of flow as the head loss is greater in the diffuser direction. For smaller opening angles of around < 10°, the diffuser is the positive direction of flow while the nozzle is the negative direction of flow since the head loss is larger in the nozzle direction.

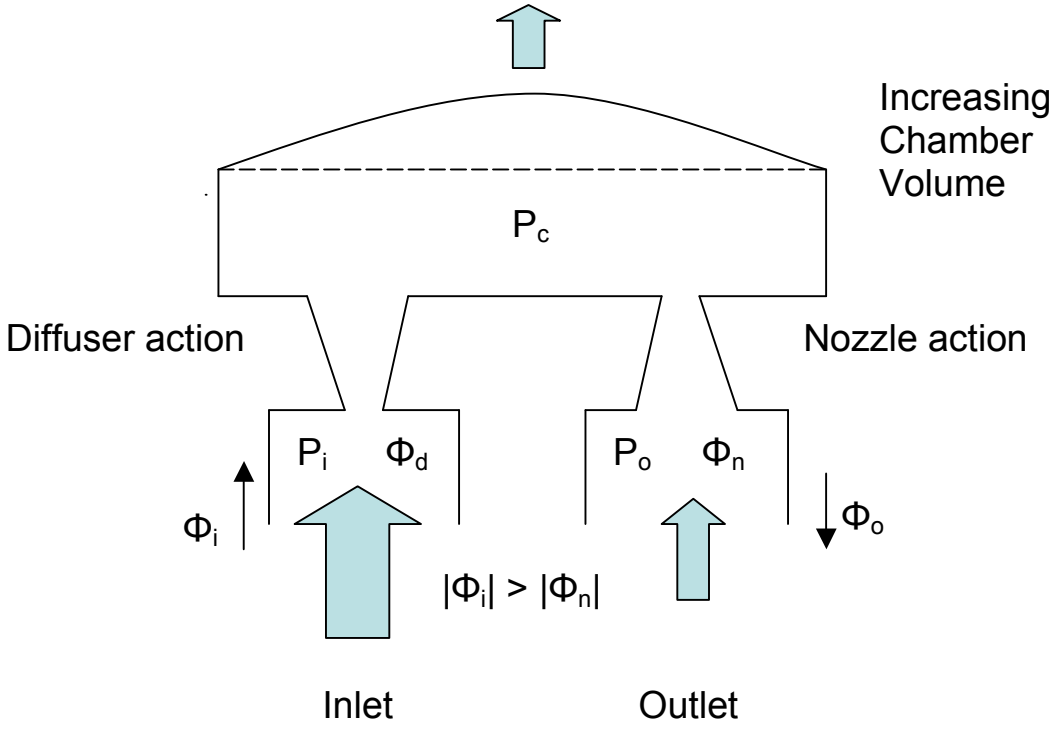

(a)

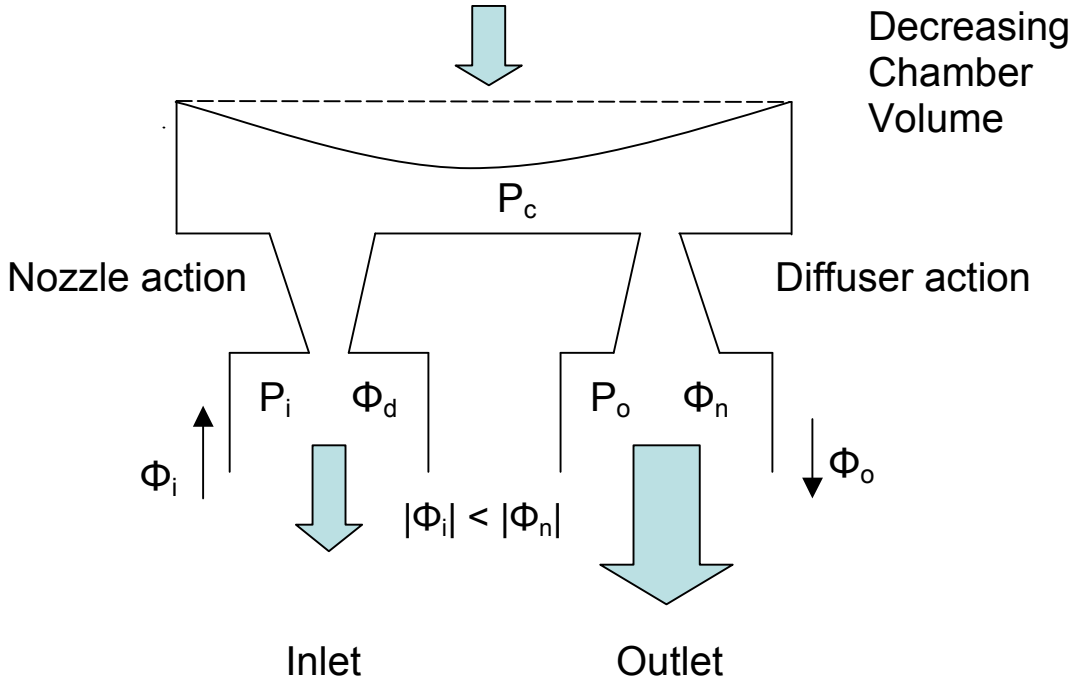

(b)

Figure 4.29 Operating of the diffuser / nozzle based pump (a) Supply mode (b) Pump mode.

The pump design presented in the present study uses diffuser / nozzle structure with smaller opening angle of around 4.7°. Since this opening angle falls in the category of small opening angles, the diffuser is the positive direction of flow and the nozzle is the negative direction of flow. This is because of the fact that a diffuser / nozzle element is geometrically designed to have a lower pressure loss in the diffuser direction than in the nozzle direction, for the same flow velocity. During the increasing chamber volume (the supply mode), the inlet element act as the diffuser, with a lower flow restriction than the outlet element, which acts as a nozzle. This means that a larger volume is transported through the inlet into the chamber than through the output, as shown in Figure 4.29 (a).

During decreasing chamber volume (the pump mode), the outlet element acts as a diffuser with a lower flow restriction than the inlet element, which acts as a nozzle. This means that a larger volume is transported through the outlet out of the chamber than through the input, as shown in Figure 4.29 (b).

The result for a complete pump cycle is therefore that a net volume is transported (i.e. pumped) from the inlet side to the outlet side, despite the fact that the diffuser / nozzle element conveys fluid in both the directions.

For describing the flow through a straight pipe, simple law of Bernoulli can be sufficient. Here the turbulence can be applied as an empirical head loss H_L. The head loss factor can be regarded as the effect of transformation of potential energy into kinetic energy as well as generation of dissipative heat [5]. All losses other than those

due to normal fluid friction can be described by the head loss factor χ, which correlates with the head loss as follows:

$$\chi = \Delta p \left(\frac{\rho}{2} \bar{u}^2 \right)^{-1}$$

Where,

Δp = pressure difference across the object

ρ = density of the fluid

$\bar{u}$ = average velocity

The flow in the nozzle direction is shown in Figure 4.30 (a). The flow enters through the inlet where it is accelerated by the sudden contraction at plane A. the head loss factor for this sudden contraction is 0.44 [5]. Then the pressure drop across the duct increases the kinetic energy and thus also the flow velocity. In the present study, where small taper angles are used, the head loss is about 0.02 [5]. Finally, the flow exits at maximum speed into a large reservoir at plane B, where the flow velocity is reduced to smaller values. This exit is referred to as sudden expansion with a head loss factor of χ_{se} = 1 [5]. The total head loss factor is calculated by summing all individual components. After summation, a total head loss factor is found out to be 1.46.

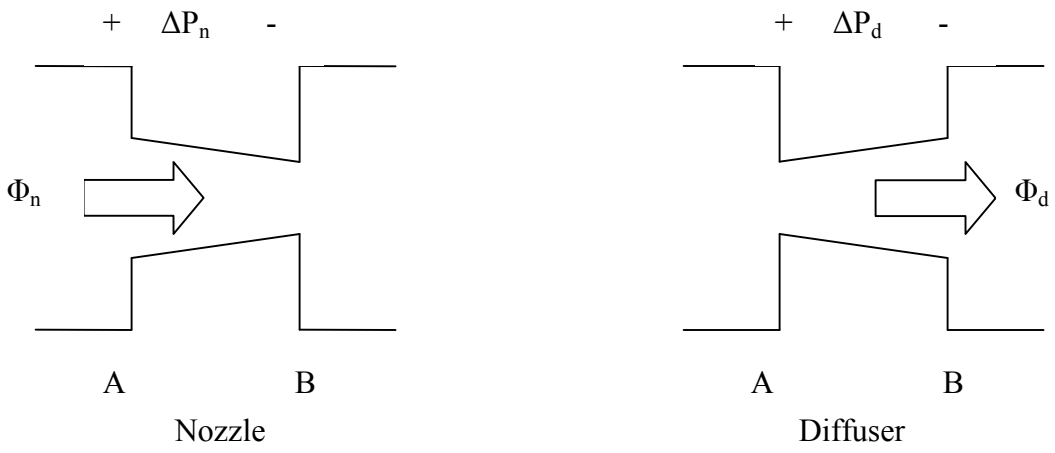

Figure 4.30 Schematic cross-section view of (a) a nozzle and (b) a diffuser.

For a flow in the diffuser direction, the fluid enters through a small opening where it undergoes sudden contraction. The head loss factor for this case is 0.44 [5]. The gradual expansion region follows where the kinetic energy is transformed into potential energy at a head loss factor of 0.3. The decelerated fluid then drains into a large reservoir by passing a sudden expansion with a head loss factor of 1. The total head loss factor for the diffuser direction is therefore 1.74. The Table 4.6 summarizes the head loss factors for the flow in the diffuser and nozzle direction.

Table 4.6 Head loss factors in the diffuser and nozzle direction.

Direction of flow	Head loss factor due to Sudden Contraction χ_{sc}	Head loss factor due to Sudden Expansion χ_{se}	Head loss factor due to Gradual Contraction χ_{gc}	Head loss factor due to Gradual Expansion χ_{ge}	Summation of the head Loss Coefficients
Diffuser	0.44	1	X	0.3	1.74
Nozzle	0.44	1	0.02	X	1.46

The value of Σ (χ_D - χ_N) can be found out to be 0.28. There are two main sources of pressure drop across the diffuser / nozzle structure. These can be calculated by means of Hagen-Poisseuille Law and modified Bernoulli equation [5]. In the case of diffuser the pressure drop is determined by [5, 27].

$$\Delta p_{diff} = \int_0^L \frac{128 \times \mu \times \Phi_v}{\pi (D_0 + x \tan\alpha)^4} dx + \left(\chi_{sc} \frac{\rho}{2} \left(\frac{4\Phi_v}{\pi D_0^{\,2}} \right)^2 + \chi_{ge} \frac{\rho}{2} \left(\frac{4\Phi_v}{\pi D_0^{\,2}} \right)^2 + \chi_{se} \frac{\rho}{2} \left(\frac{4\Phi_v}{\pi (D_0 + L \tan\alpha)^2} \right)^2 \right)$$

Here the first part is Hagen-Poisseuille Law applied to a diverging duct and the second part is the modified Bernoulli equation i.e. sum of all additional pressure losses χ_i.

Where,

D_0 = smaller diameter of the cone

α = taper angle

Φ_v = volume flow through the devise

μ = dynamic viscosity

ρ = density of the fluid

Δp = pressure drop

L = length of the duct

Solving and simplifying the above equation gives a polynomial of second order, relating the pressure drop Δp and volume flow Φ_v:

$$\Delta p_{diff} = \frac{128 \times \mu \times \Phi_v}{3\pi \tan\alpha}\left(\frac{1}{{D_0}^3} + \frac{1}{(D_0 + L\tan\alpha)^3}\right) +$$

$$\frac{8\rho{\Phi_v}^2}{\pi^2}\left(\chi_{sc}\frac{1}{{D_0}^4} + \chi_{ge}\frac{1}{\pi{D_0}^4} + \chi_{se}\frac{1}{(D_0 + L\tan\alpha)^4}\right)$$

In the same way, an equation for the pressure as the function of the volume flow can be found out for the nozzle direction. The viscous flow for this direction is identical to that of the diffuser, but the modified Bernoulli part is responsible for a flow directing behaviour of the diffuser / nozzle structure.

$$\Delta p_{nozzle} = \frac{128 \times \mu \times \Phi_v}{3\pi \tan\alpha}\left(\frac{1}{{D_0}^3} + \frac{1}{(D_0 + L\tan\alpha)^3}\right) +$$

$$\frac{8\rho{\Phi_v}^2}{\pi^2}\left(\chi_{sc}\frac{1}{(D_0 + L\tan\alpha)^4} + \chi_{gc}\frac{1}{\pi{D_0}^4} + \chi_{se}\frac{1}{{D_0}^4}\right)$$

Figure 4.31 shows the graph of the pressure as a function of the volume flow. The dimensions taken for calculation are L = 1680 μm, D_0 = 100 μm, α = 4.76°, μ = 1.002×10^{-3} Pa s, ρ = 1000 kg/m^3. The graph should have a typical square root shape. The difference between the flows in the diffuser and the nozzle at a particular value of pressure will give the net flow rate at that pressure.

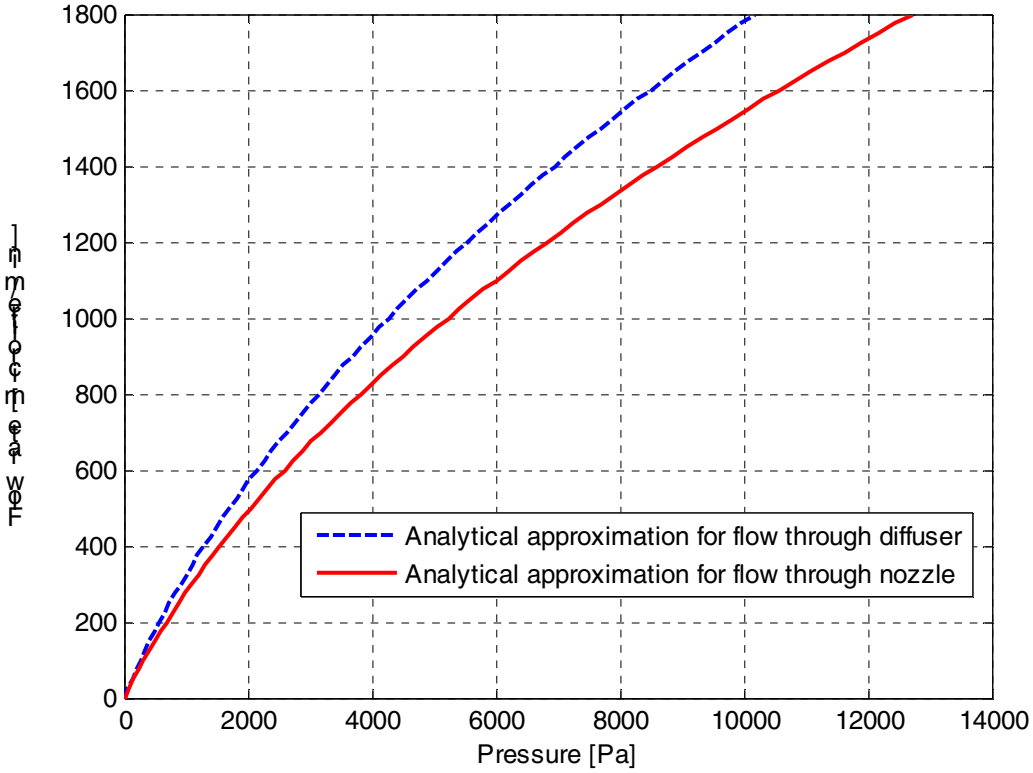

Figure 4.31 Analytical results for diffuser and nozzle at a taper angle of 4.76°.

CHAPTER V

FABRICATION

Once the final designs for the micropump were finalized, they were fabricated. Various designs for the pump were generated in LASI and were send to some external vendors for Deep Reactive Ion Etching (DRIE) process. Two types of designs were sent. One was the pump structure and the other type was various molds for Parylene deposition. Other processes required for the complete assembly of the pump were carried out at the NanoFAB Center. These other processes were thermal evaporation of the metals, Parylene-Parylene bonding, photolithography, Reactive Ion Etching (RIE), Wet etching and cleaning [8].

5.1 Parylene microtube

Parylene is used as a material to fabricate the polymer tube, which will be used in the in-plane micropump design. Our initial design reported in [17] faced issues related to leakage of fluid through the 2 μm gap provided for the free motion of the actuator parts and the diaphragm. This fluid then would reach the actuators and would stop the performance of the pump. Enclosing the fluid into a tube was the solution to this issue. Parylene was found to be a suitable material to be manufactured as a tube like structure. Parylene is a thin-film structure which can be confirmally deposited over a substrate. Other most important property of Parylene, which is of a particular

significance here, is the biocompatibility. A physical property of Parylene tube is used to achieve flexibility of the tube.

The fabrication technique of the tube presented here will provide a leak free path for the flow of fluid through it. A technique to manufacture enclosed Parylene microchannels was suggested by Noh *et. al*. [32, 36]. This was called 'Parylene micromolding'. Here, free standing Parylene microchannels were fabricated by depositing Parylene over Deep Reactive Ion Etched molds of silicon. This Parylene structure was then released by using releasing agents such as Micro-90 (Specialty Coating Systems) and Camie 1080 (Camie-Campbell Inc., St. Louis, MO). This process eliminates the expensive and time-consuming steps of photolithography. The method used the concept of molding is used to fabricate the Parylene tubes of various cross-sectional dimensions. The limitation of this process was that tubes of aspect ratio greater that 1:1 (width: height) was not easily released from the substrate.

The novel concept of chemical release of high aspect ratio Parylene microtube was proposed in our group [8]. The same concept is used in the present study. Tubes with aspect ratio of about 1:3 have been fabricated and reported in [8].

Use of Parylene as a diaphragm material is shown in [37, 40]. It was reported here that thermal residual stresses were developed because of the wet silicon etching process. In their process, first the silicon wafer was oxidized followed by corrugation generation on the wafer. Then Parylene was deposited and then the wafer was backside etched using ethylene diamine pyrocatechol (EDP). This process took place at around 70°C. Due to the difference in thermal expansion coefficients of Parylene and silicon,

thermal residual stresses were developed in Parylene which made the diaphragm difficult to deflect.

The Parylene deposition technique employed in this thesis for the modified In-plane micropump design is free of any thermal residual stresses. Parylene is evaporated over Deep Reactive Ion Etched silicon mold, which is already deposited with a layer of nickel or oxidized to form a layer of silicon dioxide. Later, this nickel or oxide layers are etched away with the help of respective enchants. This process takes place at room temperature and so no residual stresses are developed in the Parylene film.

5.1.1 Process Flow

The Parylene microtube is fabricated in two steps. The lower U shape region is fabricated separately and then it is bonded to the top portion thermally. The Deep Reactive Ion Etched (DRIE) silicon molds are used to evaporate Parylene over. This DRIE silicon is already deposited with either nickel or oxidized to form a layer of silicon dioxide. Nickel or oxide act as sacrificial layers. Nickel of around 500 °A was confirmally deposited over the DRIE mold in [8]. Later this nickel or oxide layer is etched away by respective enchants. The upper portion of the tube is formed by depositing Parylene on a glass substrate and thermally bonding this with the released Parylene from the first step. This top cover forms the cover of the tube along with the passages for fluidic connections. The process flow is explained below.

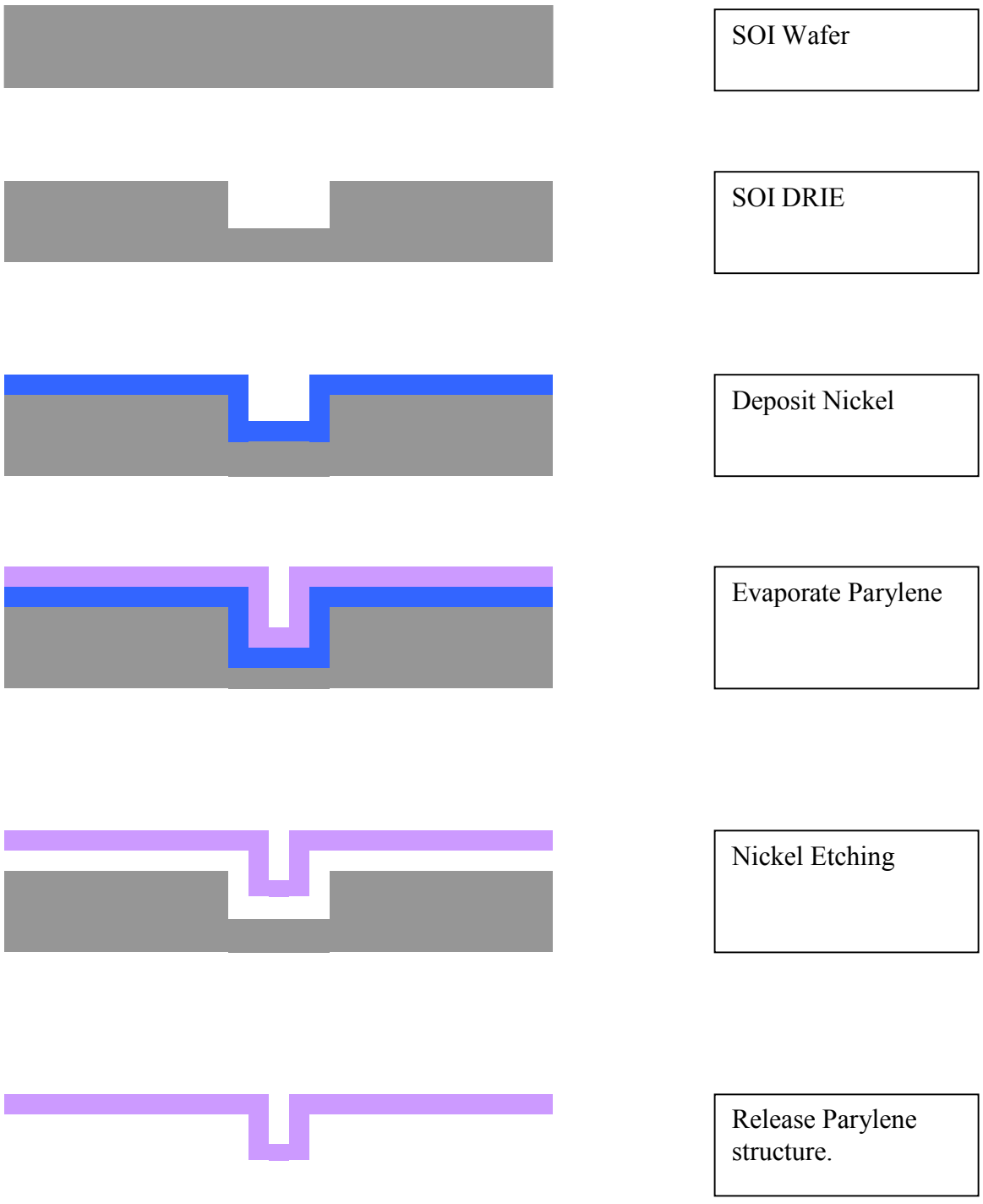

Figure 5.1 Process flow diagram for the lower portion of the Parylene microtube [8].

Figure 5.2 Colour scheme diagram of the lower portion of the Parylene microtube [8].

The second step of forming a cover for the microtube and forming fluidic connections is explained in the Figure 5.3. The glass substrate is first deposited with chrome followed by gold on both the sides of the glass. This was done in a thermal evaporator at the NanoFAB Centre. Positive photoresist will then be spincoated over this chrome+gold deposited glass surface on both the sides. The photoresist will then be patterned and developed on the top surface followed by etching the chrome+gold. Later the glass will be etched using HF. This will be done to form holes in glass at the position where there were fluidic connections. Later the photoresist will be striped using acetone followed by etching away the layer of chrome+gold. Now we will get a glass with holes where required. Now this glass substrate will be sent for Parylene deposition.

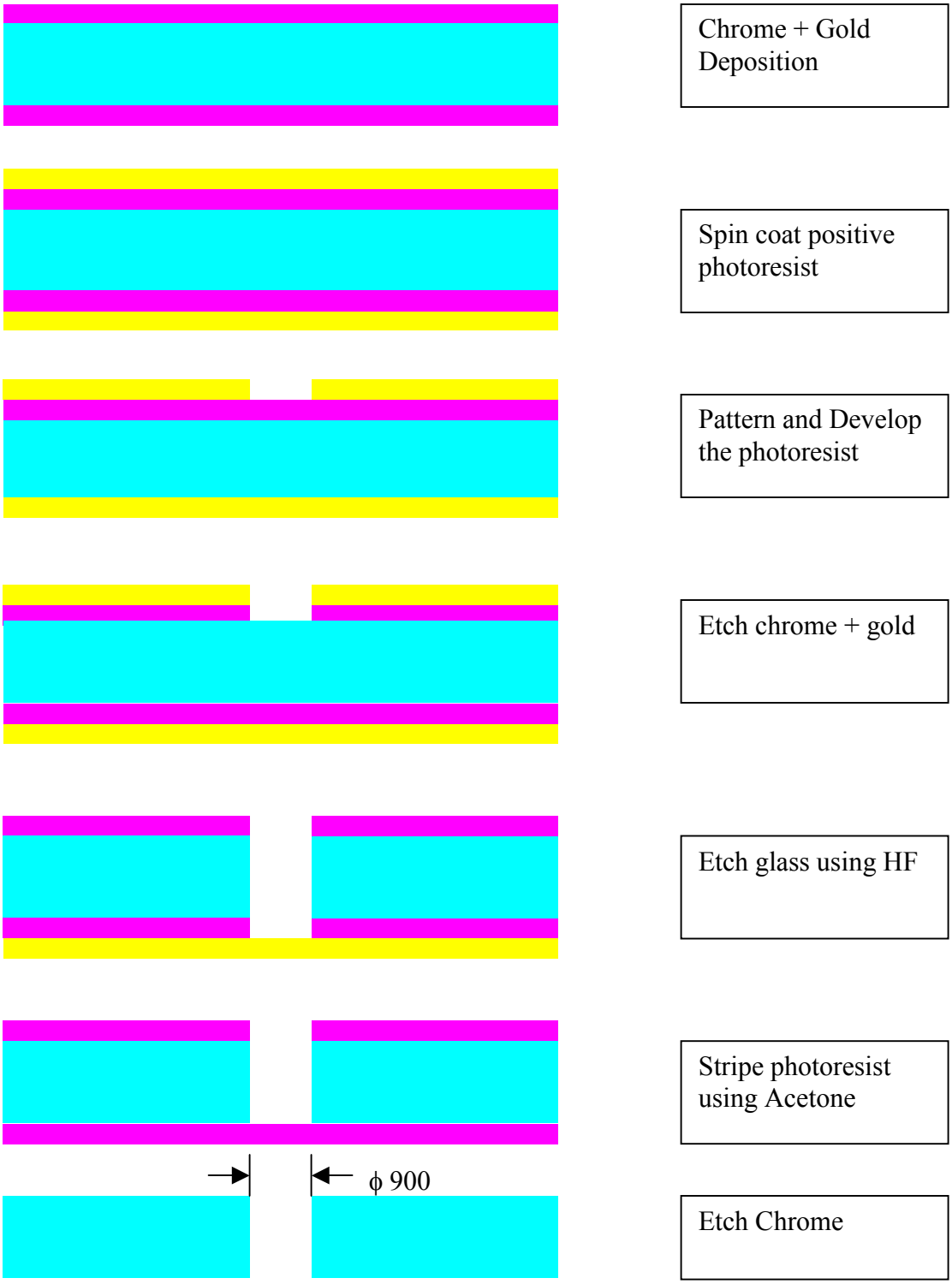

Figure 5.3 Process flow diagram for the to glass cover slide [8].

The Figure 5.4 shows the glass slide coated with Parylene. The Parylene part from first step is then thermally bonded to the Parylene coated glass in nitrogen atmosphere. This is done by aligning the silicon mold and the glass slide [8]. The alignment will be done manually under microscope. The aligned dies will be loaded into the oven for bonding. The oven has a nitrogen atmosphere. The temperature is ramped up to just below the melting temperature i.e. 290 °C in 30 minutes.

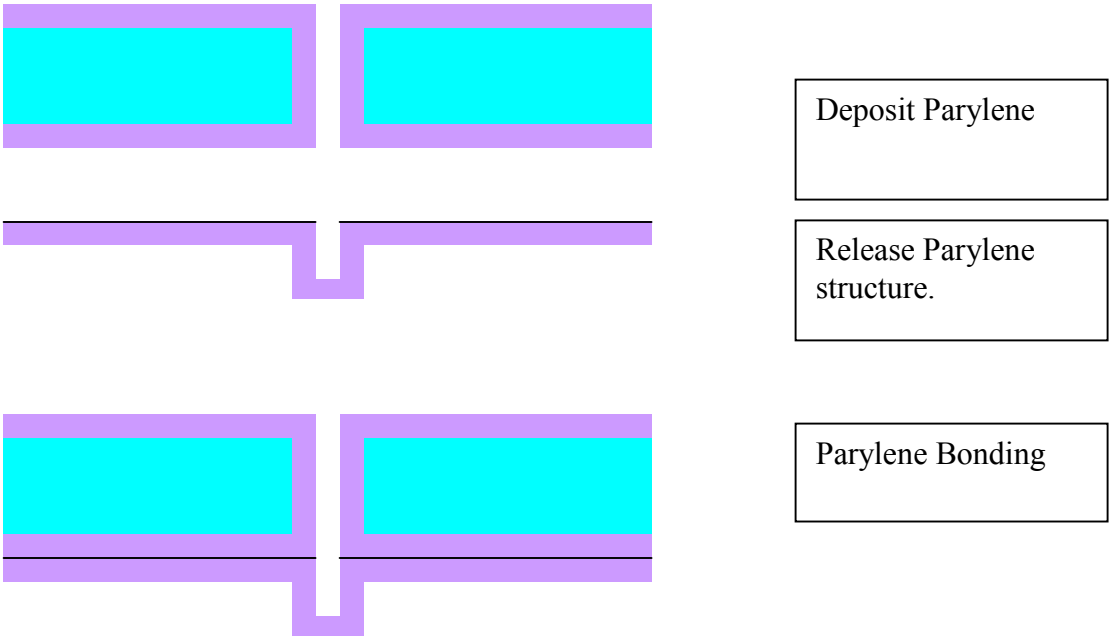

Figure 5.4 Flow process for bonding the two Parylene layers [8].

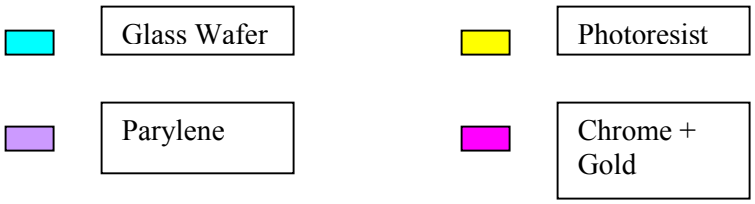

Figure 5.5: Colour scheme diagram of the Parylene Microtube [8].

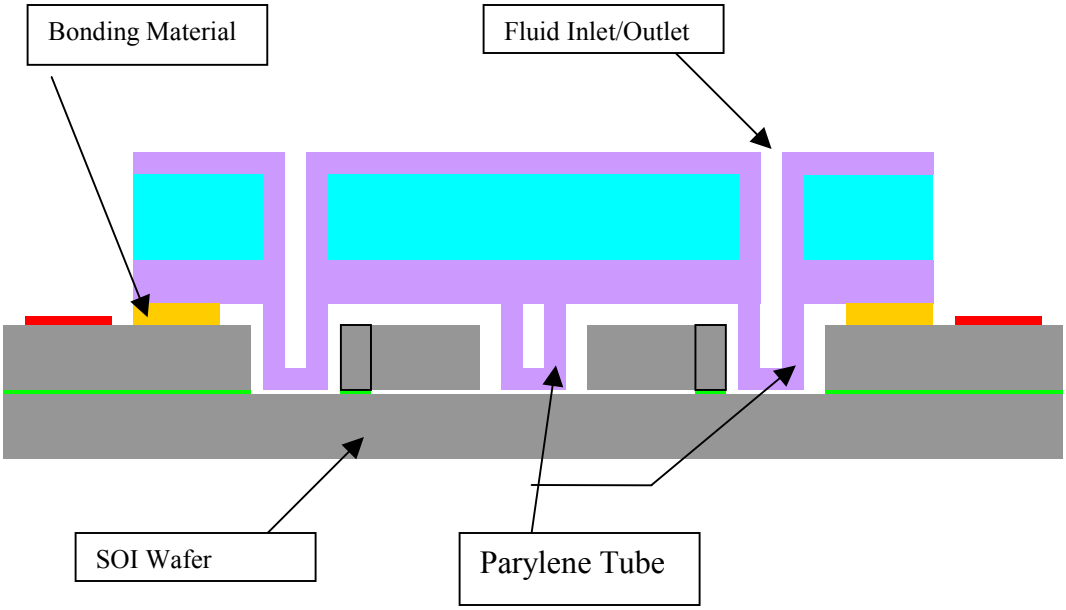

Figure 5.6 Schematic design of the micropump.

CHAPTER VI

CONCLUSION AND FUTURE WORK

6.1 Conclusions

The Chapter I of the present report introduces to the topic of microfluidics and micropumps in general and the polymer tube embedded in-plane micropump and its design optimization in particular. The Chapter gives a background and the growing treads in microfluidics. This growth is reflected in the advances made in design, analysis, characterization and fabrication of microfluidic devices such as micropumps. The present in-plane micropump design is well suited for biomedical and biochemical applications such as implantable drug delivery systems, harmful pathogen detection system, drug discovery etc. The use of polymers in microfluidic applications is illustrated in this study. The chapter explains the motivation behind this study and also the approach and the contribution of this study.

The Chapter II presents a detailed literature survey of the existing micropump actuation principles. It reports the various mechanical and non-mechanical principles which are in common use today. The various applications of the micropumps are explained here. Application of micropumps in biomedical, microelectronics cooling, chemical and biological analysis and space exploration are explained in brief. A classification of micropump actuation principles is given here. Mechanical actuation principles consist of piezoelectric, pneumatic, thermopneumatic, electrostatic,

bimetallic, shape memory and electrothermal principles. Non-mechanical actuation techniques include electrohydrodynamic, electroosmotic, ultrasonic and magnetohydrodynamic principles. Diffuser / nozzle valve principle and micropump are also presented here. This type of valve principle does not require any moving parts thus extending the life and reliability of the micropump. The section contains a brief literature review of the existing diffuser / nozzle micropumps. This Chapter also presents a survey of the type of analysis done by different researchers on the topic of micropumps in general and diffuser / nozzle micropumps in particular. Researchers have used both analytical and numerical techniques for micropump analysis. The latest trend is the extensive use of different commercial Finite Element codes for structural, fluidic, thermal, electrostatic, electromagnetic and coupled field analysis.

This Chapter introduces Parylene as a structural material in microfluidics. The chapter explains Parylene for both its traditional use and new potential applications. Applications of Parylene as a flow sensor, flow control actuator, micro check valve, in gas chromatography, and Parylene as a bonding material are explained. Parylene is introduced for its new application as a structural material. A literature review of Parylene structural analysis is presented here.

The Chapter III introduces the original in-plane micropump design. The issue of leakage through the gap is explained here. A solution is suggested in terms of use of an enclosed polymer tube for this issue. It was concluded upon a detailed survey that Parylene is a suitable to manufacture such a tube owing to is desirable mechanical

properties, biocompatibility and ease in manufacturing. A brief idea for the tube manufacturing is presented here.

The Chapter IV deals with the detailed analysis of the Parylene tube. ANSYS is used as a commercial finite Element code for this purpose. The load-deflection analysis was carried out for two different designs of the tube. The two different cross-section geometries were 100 μm × 100 μm (width × height) and 50 μm × 150 μm (width × height). It was found out that the deflection was greater for the second design case i.e. 50 μm × 150 μm (width × height) for the same load. So this design was takes as a base for further calculations. One drawback of this design was that this tube extended beyond 100 μm in height, so the lower silicon layer of the SOI structure needed to be Deep Reactive Ion Etched (DRIE) to add the trench required. This increased the cost and time for the fabrication process. Nevertheless this design was analyzed further. It was found that the maximum deflection for pressure difference of 100 kPa for a 4 μm thick Parylene tube was 2.38 μm for 100 μm × 100 μm design and was 5.42 μm for 50 μm × 150 μm design. After the deflection results were obtained, the compression ratio was calculated. A unique method to calculate the stroke volume was proposed here. It was not possible to find the stroke volume analytically owing to the complex geometry and boundary conditions. The nodal deflection results were noted from ANSYS and a 3 dimensional surface was plotted in MATLAB. The volume below that surface was found by integration. This method gave a maximum compression ratio of 0.074 for the tube thickness of 4 μm and 100 kPa of applied load.

Later the modal analysis for the tube structure was done. This was to find the natural frequency of the structure with and without considering fluid on one side of the tube. The fluid on one side will induce damping in the structure. If the first natural frequency of the structure, with and without considering fluid on one side, was less that 10 times the maximum frequency of the actuation for quasi-static consideration, a dynamic analysis would have been needed for the pump. It was concluded after the modal analysis that dynamic analysis was not needed and the quasi-static assumption was valid. ANSYS was used to calculate the modal analysis of the structure vibrating in vacuum and analytical model was used to find the natural frequency of the structure with fluid on one side.

The electrothermal actuators were used to actuate the Parylene tube. The initial design of the actuator was modified to actuate the polymer tube structure. The actuator was analyzed for the voltage-displacement and voltage-temperature results. The analysis was done using coupled elements in ANSYS. This allowed having the electrical, thermal and structural parameters as results in the analysis. It was found that the displacement and temperature increased linearly with increase in voltage. The voltage applied was from 10 V to 15 V in the step of 1 V. The maximum displacement achieved at the tube end of the actuator was 14.8 μm and the temperature reached at this end was about 400 °C. This temperature was not suitable for the Parylene tube as the melting temperature of the Parylene is 290 °C. The temperature at the tube end of the actuator needed to be reduced keeping the temperature at the V-beam same to assure the required deflection. This required a change in the structure of the actuator. So the

structure was modified by many different ways. The length of the central rod was increased to increase the path of the heat flow. The fins were attached at the top portion of the lower beams to increase the volume and the surface area for heat dissipation. The actuator was modeled with the inclusion of the already existing etch holes within the structure. This increased the surface area and the resistance for the flow of heat. Upon the above modifications, the temperature at the tube end of the actuator was seen to be significantly reduced up to 244 °C, which is less that the melting temperature of the Parylene. In practice, the temperature will be still low as the moving structure which gets heated is very close to the lower silicon substrate and the top glass cover, both of which are at ambient temperatures. So there will be a heat transfer to the top and the bottom. This effect could not be modeled in the present study due to the complexity of the analysis, number of elements required for analysis, time and memory required for the analysis.

The flow through the diffuser and the nozzle valves of the pump was analyzed. The differential flow in the two directions was a result of different pressure loss coefficients is those directions. For smaller taper angles, as in the present case, the diffuser is the positive or preferred direction of flow as compared to the nozzle.

Chapter V presents the fabrication process of the Parylene tube. Parylene, being a thin film structure, can be conformally deposited over a substrate. In the present study, Parylene was deposited on Deep Reactive Ion Etched (DRIE) structure. The novel technique of chemical release of the Parylene was used in the present study. The released Parylene was thermally bonded to the Parylene coated glass surface to form a

closed Parylene tube. This tube is then aligned and placed into the trench in the pump die. Another advantage of the present Parylene tube manufacturing technique is the thermal residual stress free deposition. This is because the Parylene is not exposed to high temperatures while manufacturing.

6.2 Future Work

Major research topics to further study this research work include:

1. A detail Fluid-Structure analysis of the Parylene tube and the fluid enclosed. This can be done statically. The analysis is required to get an in depth feel of the behavior of the Parylene structure after application of load.

2. To develop an empirical formula to find the relationship between deflection and stroke volume for a particular thickness to avoid going through the complicated and time consuming process of compression ratio calculation incorporated in the present study.

3. A more realistic modeling of the electrothermal actuator is needed to find the accurate temperature distribution and deflection. The structure should still be modified to reduce the temperature at the tube end to a lowest possible value. Though the tube will not melt below 290 °C, thermal residual stresses will develop within the Parylene structure upon exposure to high temperatures. This will affect the deflection of the tube and also may reduce the life of the structure.

4. The dimensions of the diffuser / nozzle valves should be modified and optimized for maximum flow rectification. These modifications are easy to be done. The modifications in terms of the taper angle, length of the diffuser / nozzle elements,

end dimensions and shapes such as incorporating a curvature for minimum pressure loss etc. should be done.

5. The detailed dynamic modeling of the pump is necessary to find out the flow rate and the back pressure behavior. CFD analysis should also be done to study the transfer of heat from the actuators to the fluid. An analytical optimization should be done to quickly formulate the dimensions to suit the end flow rate or pressure conditions.

6. The further study of this pump should be done keeping in mind the ultimate end application of the device.

7. Fabrication of this device should be studied in detail to study the effect of various materials to be used for releasing the Parylene tube. Cost effectiveness of the manufacturing process should be looked into.

8. In the long term, the use of different polymers in this structure as well as broadly in microfluidics should be studied. The advantage of polymer materials such as low cost, ease in manufacturing and biocompatibility should be utilized to its maximum. Also a special consideration should be given for the use of polymers as structural materials.

REFERENCES

1. Nguyen, N. T., and Wereley, S. T., "Fundamentals & Application of Microfluidics", Artech House, 2002
2. Tay, F. E. H., "Microfluidics and BioMEMS Applications", Kulwer Academic Publishers, 2002.
3. Gravesen, P., Branebjerg, J., and Jensen, O. S., "Microfluidics – A Review", J. Micromechanics & Microengineering, 3(4), 168-182, 1993.
4. Laser, D. J., Santiago, J. G., "A review of micropumps", J. Micromechanics & Microengineering, 14(2004) R35-R64, 2004.
5. Koch, M., Evans, A., Brunnschweiler, A., "Microfluidic Technology and Applications", Research Studies Press Ltd., Baldock, Hertfirdshire, England, 2000.
6. Shoji, S., Nakagawa, S., Esashi, M., "Micropump and sample injector for integrated chemical analysis systems", Sensors and Actuators, vol. A 21, 189-192, 1990.
7. Zhang L., Koo J.M., Jiang L., Goodson K.E., Santiago J.G., Kenny T.W., "Measurements and Modeling of Two-Phase Flow in Microchannels with Nearly-Constant Heat Flux Boundary Conditions", IEEE/ASME Journal of MicroElectroMechanical Engineering, Vol. 11, pp. 12-19.

8. Bushan, K., “MEMS Microfluidic system”, Masters Thesis, Electrical Engineering, The University of Texas at Arlington, May 2005.
9. Zengerle, R., Richter, M., “Simulation of microfluidic systems”, Journal of Micromechanics and Microengineering, vol. 4, no. 4, pp. 192 – 204, 1994.
10. van de Pol, F. C. M., van Lintel, H. T. G., Elwenspoek, M., Fluitman, J. H. J., “ Thermopneumatic micropump based on micro-engineering techniques,” Sensors and Actuators, vol. A 21, no. 1 – 3, pp. 198 – 202, 1990.
11. Olsson, A., Enoksson, P., Stemme, G., Stemme, E., “A valveless planar pump isotropically etched in silicon”, in Proceedings Micromechanics Europe 1995, (Copenhagen, Denmark), pp. 120 – 123, 1995.
12. Koch, M., Harris, N., Evans, A. G. R., White, N. M., Brunnschweiler, A., “A novel micromachined pump based on thick-film piezoelectric actuation”, in Proceedings Transducers 1997, (Chicago, USA), pp 353 – 356, 1997.
13. Tu., Y. L., Milne, S. J., “A study of effect of process variables on the properties of PZT films produced by a single-layer sol-gel technique,” Journal of Material Science, vol. 30, no. 10, pp. 2507 – 2516, 1995.
14. Ansari, P. H., Safari, A., “In-situ deposition of PZT thin-films by RF magnetron sputtering”, Integrated Ferroelectrics, vol. 7, no. 1 – 4, pp. 185 – 198, 1995.
15. Zhan, G., Lo, T., Liu, L., Tsien, P., “A silicon membrane micropump with integrated bimetallic actuator”, Chinese journal of electronics, vol. 5, no. 2, pp. 29 – 35, 1996.

16. Benard, W. L., Kahn, H., Heuer, A. H., Huff, M. A., “A titanium nickel shape memory alloy actuated micropump”, in Proceedings Transducers 1997, (Chicago, USA), pp. 361 – 364, 1997.
17. Sin, J., Lee, W. H., Stephanou, H. E., “In-plane micropump: design optimization”, in Technical proceedings of the 2004 NSTI Nanotechnology conference and Trade show, vol. 1
18. Manz, A., Harrison, D. J., Verpoorte, J. C., Ludi, H., Widmer, H. M., “Integrated Electroosmotic pumps and flow manifolds for total chemical analysis systems”, in Proceedings Transducers 1991 (San Francisco, USA), pp. 939 – 941, 1991.
19. Jang, J., Lee, S. S., “Theoretical and experimental study of MHD (magnetohydrodynamic) micropumps”, Sensors and Actuators A, vol. 80, 84 2004.
20. Olsson, A., Stemme, G., Stemme, E., “A numerical design study of the valveless diffuser pump using a lumped-mass model”, Journal of Micromechanics and Microengineering, vol. 9, pp. 34 – 44, 1999.
21. Voigt, P., Schrag, G., Wachutka, G., “Electrofluidic full-system modelling of a flap valve micropump based on Kirchoffian network theory”, Sensors and Actuators, vol. A 69, pp. 97 – 105, 1998.
22. Gerlach, T., “Microdiffuser as dynamic passive valves for micropump application”, Sensors and Actuators A, vol. 69, pp. 181 – 191, 1998.

23. Ullmann, A., Fono, I., “The piezoelectric valve-less pump – improved dynamic model”, Journal of Microelectromechanical systems, vol. 11, pp. 655 – 664, 2002.
24. Koch, M., Evans, A. G. R., Brunnschweiler, A., “The dynamic micropump driven with a screen printed PZT actuator”, Journal of Micromechanics and Microengineering, vol. 8, pp. 119 – 122, 1998.
25. Stemme, E., Stemme, G., “A valveless diffuser/nozzle based fluid pump”, Sensors and Actuators A, vol. 39, pp. 159 – 167, 1993.
26. Gerlach, T., Schuenemann, M., Wurmus, H., “A new micropump principle of the reciprocating type using pyramidic microflow channels as passive valves”, Journal of Micromechanics and Microengineering, vol. 6, pp. 199 –201, 1995.
27. Heschell, M., Müllenborn, M., Bouwstra, S., “Fabrication and characterization of truly 3-D diffuser/nozzle microstructures in silicon”, Journal of Microelectromechanical systems, vol. 6, pp. 41 – 46, 1997.
28. Olsson, A., Enoksson, P., Stemme, G., Stemme, E., “Micromachined flat walled valveless diffuser pumps”, Journal of Microelectromechanical systems, vol. 6, pp. 161– 166, 1997.
29. Ullmann, A., “The piezoelectric valve-less pump – Performance enhancement analysis” Sensors and Actuators A vol.69/1, pp. 97 – 105, 1998.
30. Ullmann, A., Fono, I., “The piezoelectric valve-less pump – dynamic model”, Journal of Fluids Engineering, vol. 93, pp. 92 – 98, 2001.

31. Ullmann, A., Fono, I., "The piezoelectric valve-less pump – improved dynamic model", Journal of Microelectromechanical systems, vol. 11/6, pp. 655– 664, 2002.
32. Noh, H-S., Huang, Y., Hesketh, P. J., "Parylene micromolding, a rapid and low-cost fabrication method for Parylene microchannel", Sensors and Actuators B, vol. 102, pp. 78 – 85, 2004.
33. Pomsin-Sirirak, T. N., Tai, Y. C., Nassef, H., Ho, C. M., "Flexible Parylene actuator for micro adaptive flow control", Proceedings of IEEE MEMS – 2001, pp. 511 – 514, 2001.
34. Meng, E., Tai, Y. C., "A Parylene MEMS flow sensor array", Transducers 2003, Boston, MA, 2003.
35. Wang, X. Q., Lin, Q., Tai, Y. C., "A Parylene micro check valve", Proceedings of the 12th IEEE international Conference on Micro Electro Mechanical Systems, (MEMS '99), Florida USA, pp. 177 –182, January 17 – 21, 1999.
36. Noh, H-S., Choi, Y., Wu, C., Hesketh, P. J., Allen, M. G., "Rapid low cost parylene microchannels for microfluidic applications", The 12th International conference on Solid State Sensors, Actuators and Microsystems, pp. 798 – 801, 2003.
37. Sim, W., Kim, B., Choi, B., Park, J-O., "Thermal and load-deflection FE analysis of Parylene Diaphragms", in Technical proceedings of the 2002 NSTI Nanotechnology conference and Trade show, April 2002.

38. Feng, G-H., Kim, E. S., “Micropump based on PZT unimorph and one-way parylene valves”, Journal of Micromechanics and Microengineering, vol. 14, pp. 429 – 435, 2004
39. Noh, H-S., Moon, K-S., Cannon, A., Hesketh, P. J., Wong, C. P., “Wafer bonding using microwave heating of Parylene intermediate layers”, Journal of Micromechanics and Microengineering, vol. 14, pp. 625 – 631, 2004.
40. Sim, W. C., Kim, D., Kim, K., Kwon, K., Kim, B., Choi, B., Yang, S., Park, J., “Fabrication, Test and Simulation of a Parylene diaphragm”, Transducers '01 Eurosensors XV, Munich, Germany, pp. 1382 – 1385, 2001.
41. ANSYS Release 9.0 Documentation, ANSYS, Inc., Canonsburg, PA.
42. Olsson, A., Stemme, G., Stemme, E., “A vlave-less planer fluid pump with two pump chambers”, Sensors and Actuators A, vol. 46 – 47, pp. 549 – 556, 1995.
43. Hammad, B. K., “Characterization of smart MEMs pump by applying quasi-static model based on simulations of membrane and solid-fluid interface of microvalves”, Masters Thesis, Mechanical Engineering, The University of Texas at Arlington, December 2003.
44. Blevins, R. D., “Formulas for Natural Frequency and Mode Shape”, New York, Van Nostrand Reinhold Company, 1979.
45. Greenspon, J. E., “Vibrations of Cross-Stiffened and Sandwich Plates with Application to Underwater Sound Radiators”, J. Acoust. Soc. Am. vol. 33, pp 1485 – 1479, 1961.

46. Gerlach. T., Wurmus, H., “Working principle and performance of the dynamic micropump”, Sensors and Actuators, vol. A 50, pp. 135 – 140, 1995.

BIOGRAPHICAL INFORMATION

Ashutosh Kole graduated from Shivaji University, Kolhapur, India with a Bachelor of Engineering Degree in Mechanical Engineering in August 2002. Immediately following that, he joined The University of Texas at Arlington in Fall 2002. He undertook a Curricular Practical Training at Array Products Company LLC., Muskogee, Oklahoma in Summer 2003 and fall 2003. He began working in MEMS in Spring 2004. He joined the Automation & Robotics Research Institute as a Graduate Research Assistant in Summer 2004 and began his present research work in Fall 2004. He earned is Masters of Science degree in Mechanical Engineering in August 2005.